OPTIMAL CONTROL PROBLEMS
IN TIDAL POWER GENERATION

N.R.C. Birkett and N.K. Nichols

Numerical Analysis Report NA.8/83

This paper has been prepared for incorporation in "Industrial Numerical Analysis - Case Histories", edited by C.M. Elliot and S. McKee, to be published by Oxford University Press.

1. INTRODUCTION

2. MODEL I - OSCILLATING SYSTEM

2.1 Formulation of the Problem

2.2 Necessary Conditions for the Optimal

2.3 Solution of the Optimal Control Problem

2.4 Numerical Results

2.5 Generalizations

3. MODEL II - FLAT BASIN

3.1 Formulation of the Control Problem

3.2 Conditions for the Optimal

3.3 Numerical Solution of the Control Problem

3.4 Results

3.5 Generalizations

3.6 Conclusions

4. MODELS III-IV - DYNAMIC SYSTEMS

4.1 The Model Equations

4.2 Analysis of the Model

4.3 Necessary Conditions for the Optimal

4.4 Solution of the Optimal Control Problem

4.5 Numerical Approximations

4.6 Results

4.7 Generalizations

5. CONCLUSIONS

6. REFERENCES

1. INTRODUCTION

The possibility of harnessing tidal energy has fascinated researchers for many years. Recently, tidal power generation schemes have attracted special attention due to international pressure for the development of "alternative" energy sources. The problem of extracting power from tidal motion has been examined seriously in a number of countries, and in France a tidal power generating station has been successfully established at La Rance. In Great Britain investigation has concentrated on the production of energy from tidal flow in the Severn estuary, and a recent Government report [11] has concluded that a barrage across the River Severn could be both technically and economically feasible. As expected with such a large engineering scheme, the arguments for and against the project have been hotly debated. To evaluate the tidal power scheme accurately it is necessary to calculate both the detailed component costs and the total attainable energy output, and assessment thus poses an extremely complicated optimization problem.

In this paper we develop global techniques which use the mathematical theory of control to investigate strategies for maximizing average power production from tidal schemes. In other studies [2] [8] [11] [12] [22] energy absorption figures for such schemes are computed primarily from simple linear models of one-dimensional flow in a rectangular basin. Wilson [22] examines the optimization of plant items, but does not include dynamic effects of flow in the basin in his analysis. Count [8] derives optimal constant controllers for maximizing power output using a dynamic model with and without pumping, but in his scheme the control parameters are not allowed to vary with time. A describing function method is used by Jefferys [12] and Berry [2] to examine time-dependent controls with switches for a similar linear dynamic model, but in their work it is assumed that the flow parameters all vary harmonically with the tidal period at a single frequency. This technique is therefore limited in not taking full account of all harmonic effects and is difficult to generalize to more sophisticated system models.

In the approach which we examine here, optimal control theory is applied to the full tidal power problem, and time-dependent strategies for maximizing energy output are determined using dynamic system models. This technique allows both the nature of the estuarine flow and fixed data for items of plant, such as turbines, sluices, barrier sites etc. to be taken into account while optimizing the engineering control parameters. To illustrate this approach we develop four models of the tidal power problem, each of greater complexity and greater accuracy than the previous.

The first of these models was originally introduced by Dr. B. Count for CEGB at the initial UCINA Meeting in January, 1980, and was subsequently investigated by Mr. N. Birkett in fulfillment of the requirements for the Master of Science degree at Reading University [3]. This model does not represent tidal power schemes satisfactorily, but it does provide insight into the optimal control formulation of the problem and into appropriate solution methods. The second model more realistically describes controlled flow through a barrier but does not incorporate dynamic effects in the estuary. The system, in this case as in the first model, is represented by an ordinary differential equation, and the corresponding optimal control problems have a number of characteristics in common.

For the remaining two models, dynamic effects in the estuary basin are taken into account and partial differential system equations result. In the simpler of these cases, rectangular estuaries only are considered, so that the system coefficients are constant, while in the more sophisticated model, general estuary shapes with varying depth and cross-sectional area are treated.

Numerical methods are required for the solution of the model problems, and we discuss here the development of appropriate computational techniques for each case. Two features are treated - the numerical solution of the differential system equations and the optimization of the control functions. For each model different techniques are necessary.

Investigation of the latter three models has been carried out at Reading University under the support of an SERC CASE award with CEGB, and results are reported in full detail elsewhere [4] [5]. The feasibility of a global optimal control approach to the tidal power problem is established by this research, and further extensions of the techniques described here have been, and are continuing to be made to more realistic models, with the support of CEGB and SERC. Some preliminary results for the extended cases are given in [6].

2. MODEL I - OSCILLATING SYSTEM

2.1 Formulation of the Problem

As a simple model of power generation, we consider the output obtained from a damped oscillating system. The system acts under an applied external force which can be controlled by switching the force on or off. The objective is to select the switching policy which maximizes the energy produced by the generator.

Mathematically the output $y(t)$ of the generator is given by the scalar second-order linear system equation

$$m\ddot{y} + (n + k)\dot{y} + by = g(t) \,, \tag{1}$$

where m is a mass associated with the system, n and k are natural damping constants associated with friction and the application of an electrical load, b is a constant associated with various "spring forces" in the generating system, and $g(t)$ represents the external force providing the power. (All constants m, n, k and b are positive quantities and $b > (n + k)^2$ is assumed.) The energy E produced by the generator over time interval $[0, T]$ is given by

$$E = \int_0^T k\dot{y}^2 \, dt \,. \tag{2}$$

The power generation problem is then defined as follows:

Given the initial state $\left(y(0), \dot{y}(0)\right)$ of the system, determine the partition

$$\pi_N : 0 = t_0 < t_1 < \ldots < t_N = T$$

of the time interval $[0, T]$ which maximizes the output energy E, given by (2), over all π_N (any N), subject to the system equation (1) where

$$\begin{aligned} g(t) &= F_0 \sin \omega t, \quad \text{for } t \in [t_j, t_{j+1}], \quad j \in J \\ &= 0 \,, \qquad\qquad \text{for } t \in [t_j, t_{j+1}], \quad j \notin J \,, \end{aligned} \tag{3}$$

and J is any subset of the integers $\{0, 1, 2, \ldots, N-1\}$. The sinusoidal form of the forcing function is chosen to model the behaviour of a tidal flow force, but other forms for this function may be taken.

To apply optimal control theory we reformulate the problem by introducing a bounded scalar control function $u = u(t)$ which determines the proportion of the external force that is applied at any moment. The differential equation (1) is then scaled and rewritten as a first order system. For convenience the system parameters are also simplified and we make the following definitions:

$$x_1(t) = y(t) , \quad x_2(t) = \dot{y}(t) ,$$

$$K = n/m = k/m, \quad P^2 = b/m , \quad F_0/m = 1 .$$

It is assumed that $P \geq K > 0$.

The optimal control problem then becomes

$$\max_u E(u) = \tfrac{1}{2} \int_0^T \underline{x}^T Q\underline{x} \, dt \qquad (4)$$

subject to

$$\dot{\underline{x}} = A\underline{x} + Bu , \qquad (5)$$

$$\underline{x}(0) = \underline{x}_0 \text{ given,} \qquad (6)$$

where $\underline{x} = [x_1(t), x_2(t)]^T$ and

$$Q = \begin{bmatrix} 0 & 0 \\ 0 & 2K \end{bmatrix} , \quad A = \begin{bmatrix} 0 & 1 \\ -P^2 & -2K \end{bmatrix} , \quad B = \begin{bmatrix} 0 \\ f(t) \end{bmatrix} ,$$

with $f(t) = \sin \omega t$, $\omega < P$. Admissible controls are assumed to belong to the set U_{ad} of measurable functions on $[0, T]$ satisfying (a.e.)

$$u(t) \in \Omega \equiv [0, 1] . \qquad (7)$$

We note that for any admissible control, the system equations (5)-(6) have a unique continuous solution and that (4)-(7) forms a classical constrained "linear-quadratic" optimal control problem.

The controlled proportion $u(t)$ of the applied external force is allowed to vary over the entire closed, continuous interval $[0, 1]$. At first sight this problem is not strictly equivalent to that initially described. In the next Section, however, we derive necessary conditions for the solution which show that the optimal control $u^*(t)$ maximizing the energy E must be a "bang-bang" control, that is

$$u^* = 1 \quad \text{for} \quad t \in [t_j, t_{j+1}], \quad j \in J$$
$$= 0 \quad \text{for} \quad t \in [t_j, t_{j+1}], \quad j \notin J$$

with some choice of J. The solution of the optimal control problem is therefore equivalent to that of the problem first formulated.

2.2 Necessary conditions for the Optimal

Necessary conditions for the solution of the optimal control problem (4)-(7) can be derived using either Pontryagin's Maximum Principle or a Lagrangian argument. We begin by applying the Maximum Principle in order to establish the "bang-bang" nature of the optimal control. The following theorem provides the required result [19]:

Theorem For control u with corresponding response $\underline{x}$, satisfying (5)-(6), to be optimal, it is necessary that there exists a non-vanishing vector $(\lambda_0, \underline{\lambda}(t))$ with $\lambda_0 \geq 0$ such that if the Hamiltonian H is defined by

$$H(\underline{x}, u, \underline{\lambda}) = \lambda_0 \tfrac{1}{2}\underline{x}^T Q\underline{x} + \underline{\lambda}^T(A\underline{x} + Bu) \tag{8}$$

then $\underline{\lambda}(t)$ satisfies

$$\dot{\underline{\lambda}} = -\partial H/\partial \underline{x} \equiv -\lambda_0 Q\underline{x} - A^T\underline{\lambda} \tag{9}$$

$$\underline{\lambda}(T) = 0 . \tag{10}$$

and

$$H(\underline{x}, u, \underline{\lambda}) = \max_{v\in[0,1]} H(\underline{x}, v, \underline{\lambda}) \qquad \text{(a.e.) on } [0, T] . \tag{11}$$

We note that, given u, equations (5)-(6) and (9)-(10) together form a 2n-dimensional linear two-point boundary value problem. The optimal control u must satisfy the Maximum Principle embodied in (11), that is, u must be such that

$$\underline{\lambda}^T B u = \max_{v \in [0,1]} \underline{\lambda}^T B v \, , \quad 0 \le t \le T \, , \tag{12}$$

and, therefore, u takes the form

$$u = \begin{cases} 1 \\ 0 \end{cases} \text{if} \quad \underline{\lambda}^T B \equiv \lambda_2 f(t) \begin{cases} \ge 0 \\ < 0 \, . \end{cases} \tag{13}$$

The optimal control thus lies on the boundary of the constraint set Ω of admissible values and is therefore a "bang-bang" solution as required.

An exceptional case arises if $\underline{\lambda}^T B \equiv 0$ over any (measurable) subinterval of [0, T], called a <u>singular arc</u>. On such a subinterval u is not defined by (11), and the optimal control may take interior values with $0 < u < 1$, as determined by the condition

$$\frac{d}{dt}(\underline{\lambda}^T B) \equiv 0 \, . \tag{14}$$

A further necessary condition [7] requires, however, that in such a case

$$- \frac{\partial}{\partial u}\left\{\frac{d^2}{dt^2}(\underline{\lambda}^T B)\right\} \le 0 \tag{15}$$

must also hold for E(u) to be maximized. For problem (4)-(7) it can be shown that, provided f(t) is zero only at isolated points, then (15) cannot be satisfied along a singular arc. We conclude for this problem that the optimal solution contains no singular arcs, and is strictly "bang-bang".

Existence of an optimal solution to the control problem (4)-(7) can also be demonstrated for any continuously differentiable forcing function f(t). Since the restraint set Ω is non-empty, convex and compact, and the system equations (5) are linear in $\underline{x}$ and u, the responses $\underline{x}(t)$ satisfying (5)-(6) over all admissible controls $u(t) \in U_{ad}$ are uniformly bounded, that is

$$\max_{t\in[0,T]} |\underline{x}(t)| \le \bar{X} < \infty , \tag{16}$$

where $|\underline{x}(t)| = \left[\sum_1^n x_i^2(t)\right]^{\frac{1}{2}}$. It follows then from [17] (Theorem 1, Chapt. 1) that there exists an optimal control belonging to U_{ad}.

To solve the optimal control problem (4)-(7) we look for a piecewise constant control u such that the two-point boundary value problem (5)-(6), (9)-(10) together with (13) is satisfied. Solutions are obtained by an iterative process described in the next Section. To establish the convergence of this process the gradient behaviour of the functional E(u) is required, and it is therefore instructive to examine also the Lagrangian method of establishing necessary conditions for the optimal.

The Lagrange functional associated with the problem (4)-(7) is defined by

$$L(u) = \int_0^T \tfrac{1}{2}\underline{x}^T Q\underline{x} + \underline{\lambda}^T(A\underline{x} + Bu - \dot{\underline{x}})\, dt \tag{17}$$

where $\underline{\lambda}(t)$ are Lagrange multipliers. For an admissible control u to be optimal it is necessary that the first variation $\delta L(u, v - u)$ of the functional L is <u>negative</u> for all admissible controls v, where δL is defined to be linear with respect to $\delta u = v - u$ and such that

$$L(v) - L(u) = \delta L(u, \delta u) + o(|v - u|) , \tag{18}$$

(see [9]). If we denote the difference between responses of the system (5)-(6) to controls v and u by $\delta\underline{x}(t)$, then taking variations and using integration by parts we find that

$$L(v) - L(u) = \int_0^T \underline{\lambda}^T B\delta u + \tfrac{1}{2}\delta\underline{x}^T Q\delta\underline{x}\, dt , \tag{19}$$

where $\underline{\lambda}$ satisfies the <u>adjoint</u> equations (9)-(10), and thus

$$\delta L(u, \delta u) = \int_0^T \underline{\lambda}^T B\, \delta u\, dt .$$

Assuming that $\underline{x}(t)$ satisfies (5)-(6), then the first variation of L with respect to u equals the first variation of E and we may write

$$\delta L(u, \delta u) = \langle \underline{\nabla} E(u), \delta u \rangle , \tag{20}$$

where $\langle \cdot, \cdot \rangle$ is the inner product $\langle p, q \rangle = \int_0^T p(t)q(t)dt$ and the function space gradient $\underline{\nabla} E(u)(t) = \underline{\lambda}^T(t)B$. For the control u to be optimal, then, it is necessary that

$$\langle \underline{\nabla} E(u), v - u \rangle \equiv \int_0^T \underline{\lambda}^T B(v - u)dt \leq 0 \tag{21}$$

for all admissible controls v, and therefore u must take the piecewise constant form (13), as previously derived (see also [18]).

2.3 Solution of the Optimal Control Problem

To solve the optimal control problem (4)-(7) we use an iterative technique for determining a piecewise constant admissible control u of form (13) with corresponding response $\underline{x}$ and adjoint $\underline{\lambda}$ satisfying the system and adjoint equations (5)-(6) and (9)-(10). The iteration is described by the following:

Algorithm 1

Step 1. Choose $u^0 \in U_{ad}$, piecewise constant, such that $u^0(t) := 0$ or 1, $\forall\ t \in [0, T]$.

Set $E^{-1} := 0$.

Step 2. For $k = 0, 1, 2, \ldots$ do

Step 2.1. Solve

(i) $\dot{\underline{x}}^k = A\underline{x}^k + Bu^k, \quad \underline{x}^k(0) = \underline{x}_0$,

(ii) $\dot{\underline{\lambda}}^k = -A^T\underline{\lambda}^k - Q\underline{x}^k, \quad \underline{\lambda}^k(T) = 0$.

Step 2.2. Evaluate

$$E^k := \int_0^T \tfrac{1}{2}\underline{x}^{k\,T} Q \underline{x}^k \, dt \, .$$

Step 2.3. If $E^k - E^{k-1} < tol$ then goto Step 3.

Step 2.4. Set

$$u^{k+1} := \begin{cases} 1 & \text{if } \underline{\lambda}^T B \geq 0 \, , \\ 0 & \text{otherwise} \, . \end{cases}$$

Step 2.5. CONTINUE

Step 3. Set $u := u^k$ and STOP.

The algorithm generates a sequence of admissible controls $\{u^k\}$ for which the functionals $E^k \equiv E(u^k)$ are monotonically non-decreasing. It is easily seen from (18) that if u^{k+1} is given by Step 2.4 and $\underline{x}^{k+1}$ is the corresponding response, then

$$E^{k+1} - E^k = \int_0^T \underline{\lambda}^{k\,T} B(u^{k+1} - u^k) + \tfrac{1}{2}(\underline{x}^{k+1} - \underline{x}^k)^T Q(\underline{x}^{k+1} - \underline{x}^k) dt \geq 0 \, , \quad (22)$$

since Q is positive semi-definite. The sequence $\{E^k\}$ is also bounded, since the responses $\underline{x}^k$ satisfy (16), and therefore, there exists E^* such that $\lim_{k\to\infty} E(u^k) = E^*$. Furthermore there exists a subsequence $\{u^{k_j}\}$ of $\{u^k\}$ such that u^{k_j} converges weakly to $u^* \in U_{ad}$, since U_{ad} is weakly compact (sequentially) (see [17], Lemma 1A, Chapter 2), and $\underline{x}^{k_j}$ converges uniformly to $\underline{x}^*$, the response to u^*. It follows that $E^* = E(u^*)$, and the iteration process described by the algorithm is convergent.

It remains to show that the limiting control u^* satisfies the necessary conditions for the optimal. From the weak convergence of u^{k_j}, we have that $\underline{\lambda}^{k_j}$ converges uniformly to $\underline{\lambda}^*$, the adjoint corresponding to u^*, and therefore

$$\lim_{k_j\to\infty} \langle \underline{\nabla} E(u^{k_j}), u - u^{k_j} \rangle = \langle \underline{\nabla} E(u^*), u - u^* \rangle \quad (23)$$

for all $u \in U_{ad}$. But, by the definition of u^{k+1} and the convergence of $\{E^k\}$, we have

$$\sup_{u \in U_{ad}} \langle \underline{\nabla}E(u^k), u - u^k \rangle \le \int_0^T \underline{\lambda}^{k^T} B(u^{k+1} - u^k)dt \le E^{k+1} - E^k , \tag{24}$$

and $$\lim_{k \to \infty}(E^{k+1} - E^k) = 0 . \tag{25}$$

We conclude then that

$$\sup_{u \in U_{ad}} \langle \underline{\nabla}E(u^*), u - u^* \rangle \le 0 , \tag{26}$$

as required. We note that the algorithm could also be stopped when

$$\langle \underline{\nabla}E(u^k), u^{k+1} - u^k \rangle \equiv \int_0^T \underline{\lambda}^{k^T} B(u^{k+1} - u^k)dt < tol , \tag{27}$$

that is, when u^k is close to satisfying the necessary conditions for the optimal.

We observe that Algorithm 1 defines a function iteration, and in practice it is necessary to discretize the procedure in order to compute the iterates numerically. The interval $[0, T]$ is partitioned into N steps of length $h = T/N$, and solutions are determined at the mesh points $t_j = jh$. A finite difference technique is used in Step 2.1 to solve the state and adjoint systems, and a quadrature rule is used in Step 2.2 to evaluate the functional E^k. The differential equations are approximated on the mesh by the trapezoidal difference scheme and the functional is approximated by the trapezium rule. The state equations are integrated forward from $\underline{x}(0) = \underline{x}_0$, and the adjoint equations are then integrated backward from $\underline{\lambda}(T) = 0$. Since the system equations are linear in $\underline{x}$ and $\underline{\lambda}$, the trapezoidal scheme can be written as a one-step "explicit" method, and, since meshes with constant step-size are used, no interpolations between mesh point values are required. The discrete equations for Step 2.1 and Step 2.2 are thus given by

Step 2.1'

(i) $\underline{x}_0^k := \underline{x}(0)$,

$$\underline{x}_{j+1}^k := (I - \tfrac{1}{2}hA)^{-1}[(I + \tfrac{1}{2}hA)\underline{x}_j^k + \tfrac{1}{2}h(B_j u_j^k + B_{j+1}u_{j+1}^k)] ,$$

$j = 1, 2, \ldots, N$;

(ii) $\underline{\lambda}_N^k := 0$,

$$\underline{\lambda}_{j-1}^k := (I - \tfrac{1}{2}hA^T)^{-1}[(I + \tfrac{1}{2}hA^T)\underline{\lambda}_j^k - \tfrac{1}{2}(Q\underline{x}_j^k + Q\underline{x}_{j-1}^k)] ,$$

$j = N-1, N-2, \ldots, 1, 0$;

Step 2.2'

$$E^{k+1} := \tfrac{1}{2}h \sum_{j=0}^{N}{}'' \underline{x}_j^{k^T} Q\underline{x}_j^k ,$$

where $u_j^k \approx u^k(t_j)$, $\underline{x}_j^k \approx \underline{x}^k(t_j)$, $\underline{\lambda}_j^k \approx \underline{\lambda}^k(t_j)$ and $B_j = B(t_j)$. The discrete values of the control are determined in Step 2.4 at each point t_j of the mesh by $u_j^{k+1} = 1$ if $\underline{\lambda}_j^{k^T} B \geq 0$, and $u_j^{k+1} = 0$ otherwise.

Both numerical integrations (i) and (ii) are absolutely stable since the eigenvalues μ_i of A are just $\mu_{1,2} = -K \pm i\sqrt{P^2 - K^2}$, and therefore $Re(\mu_i) < 0$, which is sufficient for absolute stability [16]. The scheme is only second-order, but since very little storage is required, and the computations are simple, it is feasible to take very small step-sizes in order to achieve high accuracy.

2.4 Numerical Results

The numerical procedures were tested for various choices of the parameters P, K and also for different choices of the forcing function $f(t)$. In most calculations the value of T was taken to be π, and the initial approximation was chosen to be $u^0 = 1$ on $[0, T]$, so that the result from the first iteration corresponded to the uncontrolled system. Experiments were also performed with initial approximations containing up to 100 switch points, in order to determine whether the converged results were affected by the starting choice.

In all cases tested the numerical value of the functional $E(u)$ increased at every iteration until consistent values were obtained, and the switch points, which essentially determine the solution, were also seen to converge. These results are illustrated in Table 1 for the case $P = 2$, $K = 1$, $\underline{x}_0 = \underline{0}$, $f(t) = \sin t$, $h = \pi/800$. Solutions in all cases were computed for a decreasing sequence of mesh sizes h. Convergence was observed and consistency was achieved for sufficiently small h (with a sufficient number of iterations for convergence of the functional). Table 2 shows the converged values of $\dot{E}$ for various meshes with N steps, together with the number of iterations required for convergence.

It was also found that the initial choice u did not affect the final result of the iterations and that the qualitative behaviour of the numerical solutions was as expected. In Figures 1 and 2 solution curves are shown for different values of P and K with $f(t) = \sin t$. In the first case the optimal control contains only two switch points, but in the second case, where $P >> K$, the optimal control switches on and off at approximately the same frequency as the natural frequency of the state system ($P/2\pi$ cycles per unit time). Similar behaviour is seen in Figure 3, which shows solution curves for the same system with forcing function $f(t) = \sin t + \frac{1}{2} \sin 2t + \sin 3t$. This type of behaviour agrees with the intuitive expectation that the control should exploit resonance effects in order to obtain maximum energy.

The most significant conclusion regarding power generation that can be reached from these results is that the energy which can be extracted from an oscillating system of type (1) can be more than doubled with the use of an appropriate control strategy. In Table 3 the energy from the uncontrolled and optimally controlled systems for various P, K and $f(t) = \sin t$ are shown. For the simple harmonic forcing function large improvements can be made in the maximum average energy produced; similar, but smaller

Table 1. Convergence of Iteration

$P = 2, \quad K = 1, \quad h = \pi/800$

Iteration no.	$E(u^k)$	Switch points t_1	t_2
k = 0	0.593	0	0
1	0.1011	0.0490	2.2044
2	0.1035	0.5541	2.1306
3	0.1039	0.5751	2.1003
.	.	.	.
.	.	.	.
8	0.1041	0.5768	2.0711
9	0.1041	0.5746	2.0707
10	0.1041	0.5746	2.0707

Table 2. Convergence of Discretization

$P = 2, \quad K = 1$

No. of Mesh Steps	$E(u^*)$	No. of Iterations
100	0.1025	6
200	0.1034	6
400	0.1038	8
800	0.1041	10
1600	0.1042	12

Table 3. Comparison of Energy Production

P	K	E uncontrolled	E optimal
2	1	0.0593	0.1042
10	1	0.0002	0.0472
20	2	0.00002	0.0330
2	2	0.0515	0.0750
4	4	0.0132	0.0269
10	10	0.0013	0.0036

FIG. 1 MODEL I

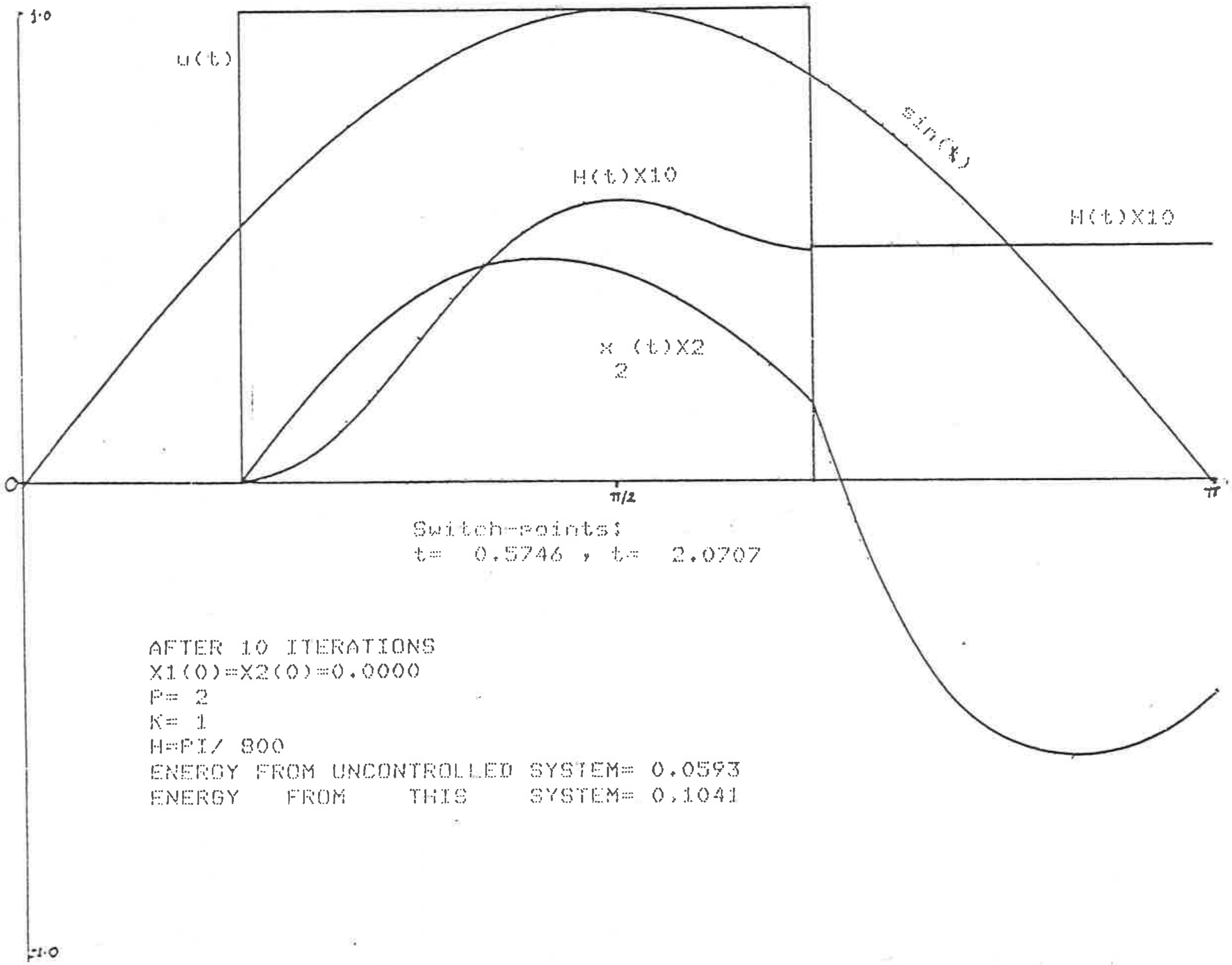
1·0
-1·0
0
π/2
π
u(t)
sin(t)
H(t)X10
H(t)X10
x (t)X2
2
Switch-points:
t= 0.5746 , t= 2.0707
AFTER 10 ITERATIONS
X1(0)=X2(0)=0.0000
P= 2
K= 1
H=PI/ 800
ENERGY FROM UNCONTROLLED SYSTEM= 0.0593
ENERGY FROM THIS SYSTEM= 0.1041

FIG. 2 MODEL I

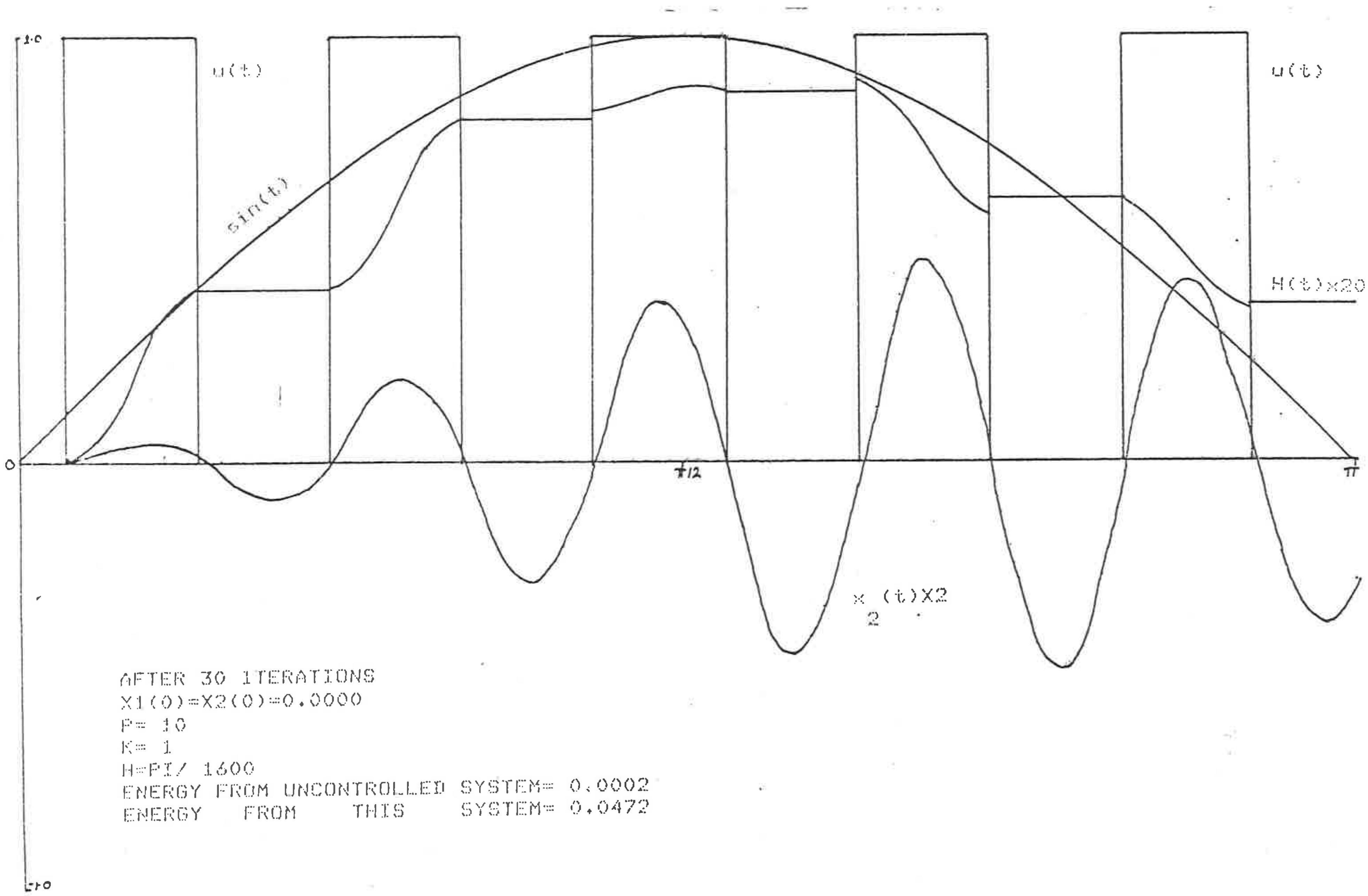
1.0
u(t)
u(t)
sin(t)
H(t)x20
0
π/2
π
x (t)X2
2
-1.0
AFTER 30 ITERATIONS
X1(0)=X2(0)=0.0000
P= 10
K= 1
H=PI/ 1600
ENERGY FROM UNCONTROLLED SYSTEM= 0.0002
ENERGY FROM THIS SYSTEM= 0.0472

FIG. 3 MODEL I - $f(t) = \sin t + \frac{1}{2} \sin 2t + \sin 3t$

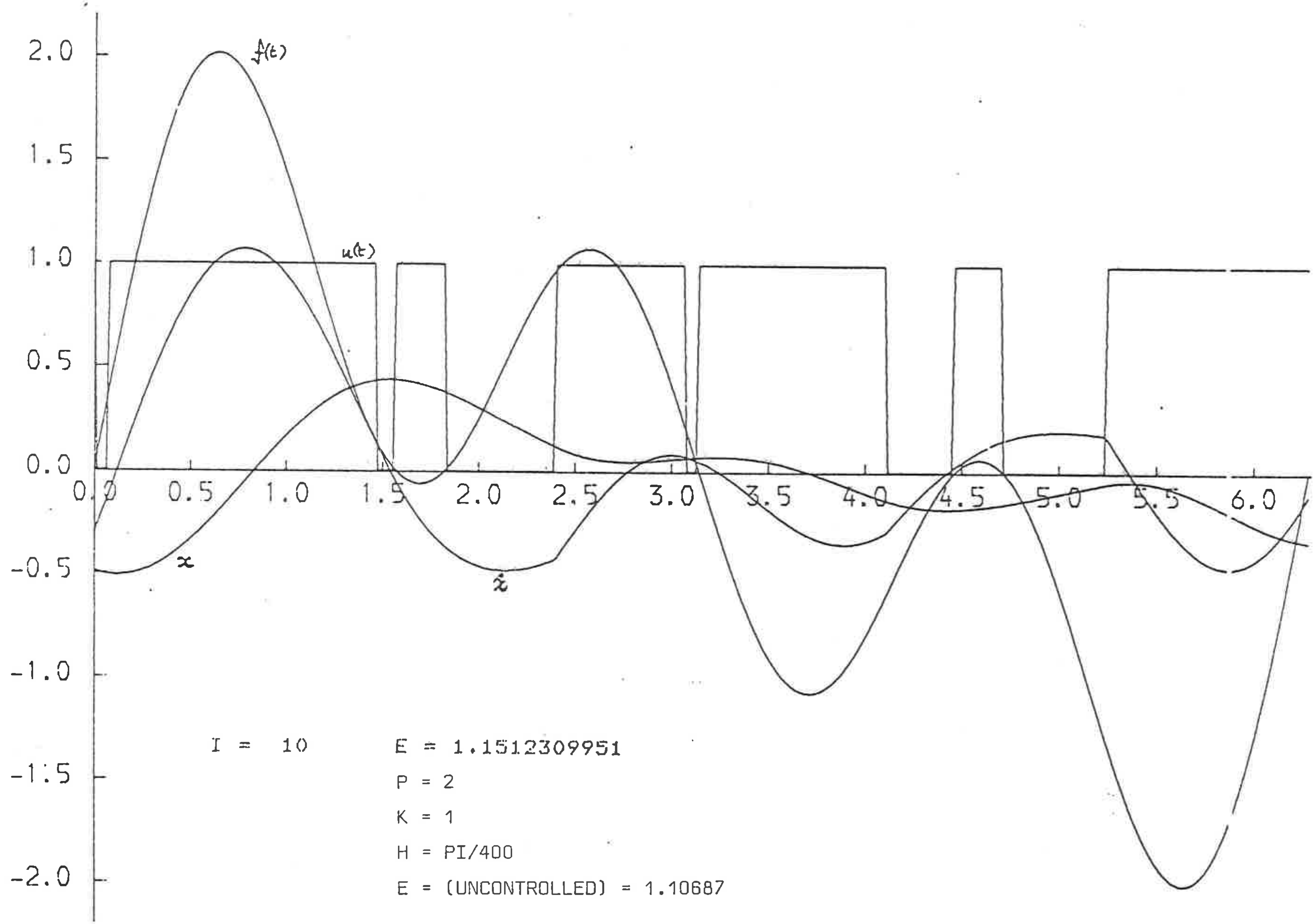

improvements, are achievable for less regular forcing functions.

2.5 Generalizations

The optimal control problem (4)-(7) discussed in the previous sections is a linear-quadratic problem with a single input, that is, a scalar control. All of the theory and numerical procedures developed for this case also apply to the general multi-input optimization problem

$$\max_{\underline{u}} E(\underline{u}) = \tfrac{1}{2}\int_0^T \underline{x}^T Q \underline{x}\, dt \,, \tag{4'}$$

subject to system equations

$$\dot{\underline{x}} = A\underline{x} + B\underline{u}, \quad \underline{x}(0) = \underline{x}_0 \,, \tag{5')-(6'}$$

where Q is positive semi-definite, $B = B(t)$ is a continuously differentiable matrix function of full rank for all t, and $\underline{u}$ is an m-dimensional measurable control vector $(m \leq n)$ on $[0, T]$ such that (a.e.)

$$0 \leq u_i(t) \leq 1 \,, \quad i = 1, 2, \ldots, m \,. \tag{7'}$$

The necessary conditions imply that the optimal control is component-wise "bang-bang" in nature, and the switches occur where the corresponding components of $\underline{\nabla E}(\underline{u})$ change sign. (There are no singular arcs, provided $B^T QB$ is singular only at isolated points.) The techniques developed are applicable, therefore, to a wide range of general problems.

3. MODEL II - FLAT BASIN

3.1 Formulation of the Control Problem

The oscillating system model described in §2 provides insight into the formulation and solution of optimal control problems in power generation, and shows that energy extraction can be greatly enhanced by the use of an appropriate control strategy. This model does not, however, represent satisfactorily a tidal power generating system in which energy is extracted from flow across a barrier.

To model the tidal power problem we start with a simple one-dimensional system consisting of an estuary with a barrier at the origin, and a basin upstream of the barrier, as shown in Figure 4. The surface elevation above mean height is assumed constant throughout the basin at any point in time; that is, dynamic effects in the basin are ignored and the basin surface is assumed to remain flat. Flow is permitted across the barrier, through turbines only, and the influx velocity is assumed proportional to the head difference between the tidal elevation on the seaward side of the barrier and the surface elevation in the basin. The control determines the proportional discharge across the available turbines.

Mathematically, then, the influx velocity u_0 is given by

$$u_0 = \alpha(t)[f(t) - \eta(t)] \ , \qquad (28)$$

where $\alpha(t)$ is the influx control, which is bounded such that $0 \leq \alpha \leq a_0$ for all t, $\eta(t)$ is the basin elevation above mean and $f(t)$ is the tidal elevation above mean. By the laws of conservation we must also have

$$u_0 = \ell\dot{\eta}(t)/h \ , \qquad (29)$$

where ℓ is the length of the basin and h is the mean depth in the basin. Solutions of the system equations (28)-(29) may be determined over any interval $[0, T]$, starting from any initial state of the system. For the tidal problem we are specifically interested in a tidal period, however,

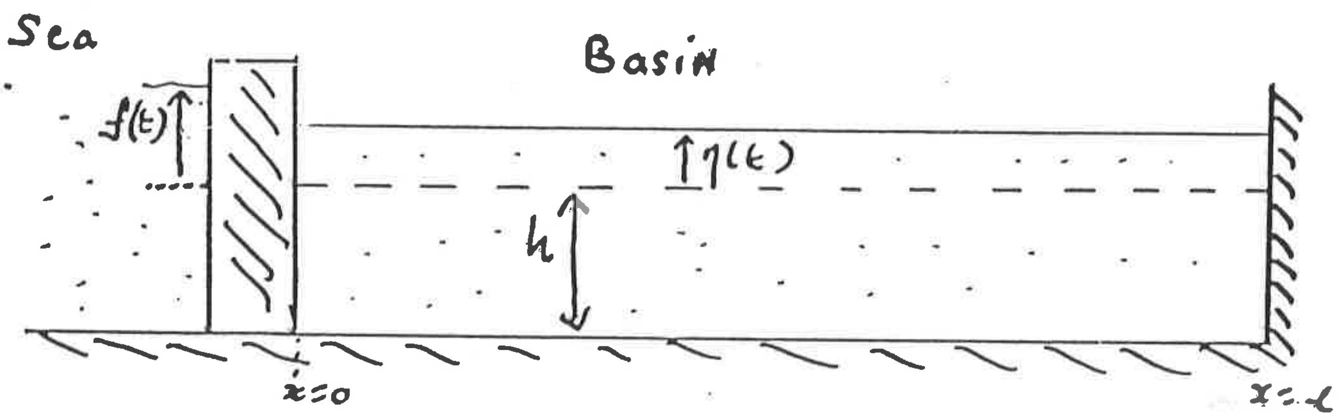

FIG. 4 - Tidal Basin

where the forcing $f(t)$ is a dominant harmonic of form

$$f(t) = F_0 \cos \omega t , \quad \omega = 2\pi/T , \tag{30}$$

with period $T \approx 12 \times 3600$s. We therefore expect to find "steady-state" solutions to the system equations which are also periodic on $[0, T]$, and we impose the boundary conditions $\eta(0) = \eta(T)$ on the problem.

The instantaneous power output from the turbines is assumed proportional to the flow times the head difference, that is, $\propto u_0[f(t) - \eta(t)]$, and the average power generated over time interval $[0, T]$ is therefore given by

$$\overline{P} = \rho g \frac{S}{T} \int_0^T \alpha(t)[f(t) - \eta(t)]^2 \, dt , \tag{31}$$

where S is the surface area of the barrier, g is gravitational acceleration and ρ is the fluid density.

The optimal control problem is then to determine the control $\alpha(t)$ which maximizes the average power $\overline{P}$ subject to the system equations and boundary conditions. The equations may be normalized with respect to time, and the optimization problem is then given by

$$\max_{\alpha \in U_{ad}} E(\alpha) = \int_0^1 \alpha(t)[f(t) - \eta(t)]^2 \, dt , \tag{32}$$

subject to

$$\dot{\eta} = K\alpha(t)[f - \eta] , \quad K = hT/\ell , \tag{33}$$

$$\eta(0) = \eta(1) , \tag{34}$$

where U_{ad} is the set of measurable functions $\alpha(t)$ on $[0, 1]$ such that (a.e.)

$$\alpha(t) \in \Omega \equiv [0, a_0] . \tag{35}$$

3.2 Conditions for the Optimal

For the control problem (32)-(35) to be well-posed, it is necessary that, for any given admissible control function $\alpha(t) \in U_{ad}$, the system equation

(33) together with boundary condition (34) must have a unique solution, continuously dependent on the data of the problem. If this can be shown, then necessary conditions for the optimal can be derived using the Maximum Principle or the Lagrange technique, and the existence of an optimal control $\alpha^*(t) \in U_{ad}$ can be established by the same arguments as used for the oscillating system in §2.

The system equation (33) is linear in the state variable $\eta(t)$ and it is easily demonstrated, therefore, that for any $\alpha(t) \in U_{ad}$ with $\int_0^1 \alpha(s)ds > 0$, that is $\alpha(t) \not\equiv 0$, the unique solution of (33) is given by

$$\eta(t) = \frac{\phi(t)}{1 - \phi(1)} \int_0^1 \phi(1)\phi^{-1}(s)K\alpha(s)f(s)ds + \phi(t) \int_0^t \phi^{-1}(s)K\alpha(s)f(s)ds \tag{36}$$

where $\phi(t) = \exp(-\int_0^t K\alpha(s)ds)$. The case $\alpha \equiv 0$ is trivial in the sense that no fluid crosses the barrier and no power is generated, and it may thus be disregarded. From the expression (36), it follows that if the forcing function $f(t)$ is continuously differentiable and bounded on $[0, 1]$, then the response $\eta(t)$ of the system (33) is uniformly bounded over all non-trivial $\alpha \in U_{ad}$ (see [4]), and a (non-trivial) optimal control belonging to the set of admissible controls exists.

From the Maximum Principle we find that a necessary condition for an admissible control $\alpha(t)$ and its response $\eta(t)$ to be optimal is the existence of an adjoint $\lambda(t)$ satisfying

$$\dot{\lambda} = K\alpha(t)\lambda + 2\alpha(t)[f(t) - \eta(t)] \tag{37}$$

$$\lambda(0) = \lambda(1) \tag{38}$$

and such that

$$H = \alpha[f - \eta]^2 + \lambda K\alpha[f - \eta]$$

is maximized with respect to $\alpha \in \Omega$ for $t \in [0, 1]$. Hence the optimal is "bang-bang" in nature and is given by

$$\alpha(t) = \begin{cases} a_0 & \text{if } [f - \eta]^2 + K\lambda[f - \eta] \geq 0 , \\ 0 & \text{otherwise} . \end{cases} \tag{39}$$

The Lagrangian for problem (32)-(35) is defined by

$$L(\alpha) = \int_0^1 \alpha[f - \eta]^2 + \lambda(K\alpha[f - \eta] - \dot{\eta})\, dt \tag{40}$$

and, taking variations, we find that if $\eta(t)$ and $\lambda(t)$ satisfy the system and adjoint equations (33)-(34) and (37)-(38), then

$$L(\beta)-L(\alpha) = \int_0^1 ([f - \eta]^2 + K\lambda[f - \eta])\delta\alpha$$

$$- (2[f - \eta] + K\lambda)\delta\alpha\delta\eta + \alpha(\delta\eta)^2 + \delta\alpha(\delta\eta)^2\, dt \tag{41}$$

where β is any non-trivial admissible control, $\delta\alpha = \beta - \alpha$ and $\delta\eta$ is the difference between the responses to controls β and α. The first variation is therefore given by

$$\delta L \equiv \langle\nabla E(\alpha), \; \beta - \alpha\rangle = \int_0^1 ([f - \eta]^2 + K\lambda[f - \eta])(\beta - \alpha)dt \tag{42}$$

which is non-positive for all $\beta \in U_{ad}$ only if $\alpha(t)$ satisfies (39). The optimal control must, thus, be piecewise constant with values at the extremes of the constraint set Ω and switches at zeros of the function space gradient

$$\nabla E(\alpha) = [f - \eta]^2 + K\lambda[f - \eta] . \tag{43}$$

We note that provided the derivative of the forcing function, $\dot{f}(t)$, has only isolated zeros, the optimal solution can contain no singular arcs, since $\nabla E(\alpha) \equiv 0$ over some sub-interval of $[0, T]$ implies that either $\dot{f} \equiv 0$, or $f \equiv \eta$ and therefore, from (33) $\dot{\eta} \equiv 0 \equiv \dot{f}$, on that sub-interval, which contradicts the assumption on $\dot{f}$. The existence and general "bang-bang" nature of the optimal control is thus established.

3.3 Numerical Solution of the Control Problem

To determine an admissible control $u(t)$ with corresponding response $\eta(t)$ and adjoint $\lambda(t)$ satisfying the necessary conditions (33)-(34), and (37)-(39), we again use an iterative technique similar to that defined by Algorithm 1. If we have an approximation α^k to the optimal control, with response and adjoint η^k, λ^k satisfying the system and adjoint equations (33)-(34) and (37)-(38), then we may choose a new approximation

$$\tilde{\alpha}^{k+1} := a_0 \quad \text{if} \quad \nabla E(\alpha^k) \geq 0 \qquad (44)$$

$$:= 0 \quad \text{otherwise,}$$

where $\nabla E(\alpha)$ is given by (43). This selection maximizes the first variation $<\nabla E(\alpha^k), \tilde{\alpha}^{k+1} - \alpha^k>$ of the functional (32) over all possible choices for $\tilde{\alpha}^{k+1}$. The energy functional (32) is not now quadratic, however, and it can be seen from (41) that $E(\tilde{\alpha}^{k+1}) - E(\alpha^k) \equiv L(\tilde{\alpha}^{k+1}) - L(\alpha^k)$ is not necessarily non-negative for this choice of $\tilde{\alpha}^{k+1}$. It can be shown, however, that there does exist an admissible control $\alpha^{k+1} = \alpha^k + \theta(\tilde{\alpha}^{k+1} - \alpha^k)$ for some $\theta \in [0, 1]$ such that $E(\alpha^{k+1}) \geq E(\alpha^k)$ (see [10]). We can therefore construct a sequence of controls $\{\alpha^k\}$ for which the functionals $E^k = E(\alpha^k)$ are monotonically non-decreasing. Since the responses η^k are continuously dependent on the controls α^k and are uniformly bounded for all (non-trivial) $\alpha \in U_{ad}$, we can again show that the sequence $\{E^k\}$ is bounded and convergent. As in the case of the oscillating system, there also exists a subsequence of the controls which converges weakly to a (non-trivial) limit $\alpha^* \in U_{ad}$ such that

$$\lim_{k\to\infty} E^k = E(\alpha^*) , \qquad (45)$$

and

$$\sup_{\alpha\in U_{ad}} <\nabla E(\alpha^*), \alpha - \alpha^*> \leq 0 , \qquad (46)$$

for all admissible controls α, and α^* satisfies the necessary conditions for the optimal.

In order to obtain periodic solutions to the state and adjoint equations

(33) and (37) for each α^k, inner iteration procedures are used. We define the processes

$$\eta^{m+1}(0) = \eta^m(1) \equiv F\{\eta^m(0)\} , \quad m = 0, 1, 2, \ldots , \tag{47}$$

$$\lambda^{r+1}(1) = \lambda^r(0) \equiv G(\lambda^r(1)) , \quad r = 0, 1, 2, \ldots , \tag{48}$$

where $F(\eta(0))$ and $G(\lambda(1))$ are the solutions of the differential equations (33) and (37) with given initial data $\eta(0)$ at $t = 0$ and $\lambda(1)$ at $t = 1$, respectively. The operators F, G can be written

$$F\{\eta(0)\} = \phi(1)\eta(0) + \int_0^1 \phi(1)\phi^{-1}(s)\alpha(s)f(s)ds , \tag{49}$$

$$G(\lambda(1)) = \psi(0)\lambda(1) + \int_0^1 \psi(0)\psi^{-1}(s)2\alpha(s)\big(f(s) - \eta(s)\big)ds , \tag{50}$$

where $\phi(t) = \exp\left(-\int_0^t K\alpha(s)ds\right)$ and $\psi(t) = \exp\left(-\int_t^1 K\alpha(s)ds\right)$, and it can be seen that since

$$|F(v) - F(w)| \le \phi(1)|v - w| , \quad 0 < \phi(1) < 1 , \tag{51}$$

$$|G(v) - G(w)| \le \psi(0)|v - w| , \quad 0 < \psi(0) < 1 , \tag{52}$$

the operators F and G are both contractions (see [13]). The iterations (47) and (48), therefore, both converge to the unique fixed points η_0, λ_1 of the operators, and the solutions of the equations (33), (37) with initial data $\eta(0) = \eta_0$, $\lambda(1) = \lambda_1$ thus also satisfy the periodic boundary conditions

$$\eta(1) = F(\eta_0) = \eta_0 = \eta(0), \quad \lambda(0) = G(\lambda_1) = \lambda_1 = \lambda(1) . \tag{53}$$

The complete function iteration procedure for determining the optimal control is described by the following:

Algorithm 2

Step 1. Choose $\alpha^o \in U_{ad}$, piecewise constant such that $\alpha^o = 0$, or a_0, $\forall\ t \in [0, 1]$.

Choose $\eta^o(0)$, $\lambda^o(1)$.

Set $\theta := 1$, $E^o := 0$, $\tilde{\alpha}^1 := \alpha^o$.

Step 2. For k: = 1, 2, ... do

Step 2.1. Set $\alpha^k := \alpha^{k-1} + \theta(\tilde{\alpha}^k - \alpha^{k-1})$.

Step 2.2. Set $\tilde{\eta}^o(1) := \eta^{k-1}(0), \quad \tilde{\lambda}^o(0) := \lambda^{k-1}(1)$.

Step 2.3. For m: = 1, 2, ... do

Step 2.3.1. Solve $\dot{\tilde{\eta}}^m = K\alpha^k[f - \tilde{\eta}^m], \quad \tilde{\eta}^m(0) = \tilde{\eta}^{m-1}(1)$.

Step 2.3.2. If $|\tilde{\eta}^m(1) - \tilde{\eta}^{m-1}(1)| < tol$ then set $\eta^k \equiv \tilde{\eta}^m$

and goto Step 2.4.

Step 2.3.3. CONTINUE.

Step 2.4. For m: = 1, 2, ... do

Step 2.4.1. Solve $\dot{\tilde{\lambda}}^m = K\alpha^k\tilde{\lambda}^m + 2\alpha^k[f - \eta^k], \ \tilde{\lambda}^m(1) = \tilde{\lambda}^{m-1}(0)$.

Step 2.4.2. If $|\tilde{\lambda}^m(0) - \tilde{\lambda}^{m-1}(0)| < tol$

then set $\lambda^k \equiv \tilde{\lambda}^m$ and goto Step 2.5.

Step 2.4.3. CONTINUE.

Step 2.5. Evaluate

$$\nabla E^k := [f - \eta^k]^2 + K\lambda^k[f - \eta^k] ,$$

$$E^k := \int_0^1 \alpha^k[f - \eta^k]dt .$$

Step 2.6. Set $\tilde{\alpha}^{k+1} := \begin{cases} 1 & \text{if } \nabla E^k \geq 0 , \\ 0 & \text{otherwise} . \end{cases}$

Step 2.7. If $<\nabla E^k, \tilde{\alpha}^{k+1} - \alpha^k> < tol$ then goto Step 3.

Step 2.8. If $E^k \leq E^{k-1}$ then set $\theta := \theta/2$ and goto Step 2.1.

Step 2.9. CONTINUE.

Step 3. Set $\alpha := \alpha^k$ and STOP.

In practice the function iteration described by Algorithm 2 is replaced by a discretized process. The interval [0, 1] is divided into steps of length $h = 1/N$ and solutions are determined at mesh points $t_j = jh$. The initial value problems in Step 2.3.1 and Step 2.4.1 are solved by a finite difference method using the trapezoidal scheme, and the functionals

E^k and $\langle \nabla E^k, \tilde{\alpha}^{k+1} - \alpha^k \rangle$ are approximated in Step 2.5 and Step 2.7 by the trapezium quadrature rule. The difference approximations are given by

$$\tilde{\eta}_0^m := \tilde{\eta}_N^{m-1} , \tag{54}$$

$$\tilde{\eta}_{j+1}^m : (1+\tfrac{1}{2}Kh\alpha_{j+1}^k)^{-1}[(1-\tfrac{1}{2}Kh\alpha_j^k)\tilde{\eta}_j^m + \tfrac{1}{2}Kh(\alpha_{j+1}^k f_{j+1} + \alpha_j^k f_j)], \; j = 1,2,\ldots N$$

and

$$\tilde{\lambda}_N^m := \tilde{\lambda}_0^{m-1} \tag{55}$$

$$\tilde{\lambda}_{j-1}^m := (1+\tfrac{1}{2}Kh\alpha_{j-1}^k)^{-1}[(1-\tfrac{1}{2}Kh\alpha_j^k)\tilde{\lambda}_j^m - Kh(\alpha_{j-1}^k(f_{j-1}-\eta_{j-1}^k)+\alpha_j^k(f_j-\eta_j^k))],$$

$$j = N-1, N-2, \ldots 0$$

and the quadrature rule gives

$$E^k := h \sum_{j=0}^{N}{}'' \alpha_j^k \left|f_j - \eta_j^k\right| , \tag{56}$$

and

$$\langle \nabla E^k, \tilde{\alpha}^{k+1} - \alpha^k \rangle := h \sum_{j=0}^{N}{}'' \nabla E_j^k (\tilde{\alpha}_j^{k+1} - \alpha_j^k) , \tag{57}$$

where α_j^k, $\tilde{\alpha}_j^k$, η_j^k, λ_j^k, ∇E_j^k are approximations to the values of α^k, $\tilde{\alpha}^k$, η^k, λ^k and ∇E^k at the mesh point t_j, and $f_j = f(t_j)$. The discrete values α_j^k and $\tilde{\alpha}_j^k$ are determined in a natural way in Step 2.1 and Step 2.6.

The difference schemes (54) and (55) are both absolutely stable and the iterations of Step 2.3 and Step 2.4 both converge to the solution of discrete periodic boundary value problems which approximate the state and adjoint systems (33)-(34) and (37)-(38). The difference schemes are technically second-order, but since the first derivative of the state variable η generally contains discontinuities, we cannot expect second-order asymptotic behaviour in this case. It can be shown, however, that the schemes for this case are at least first-order accurate [4] and therefore are convergent as $h \to 0$.

3.4 Results

Solutions to the optimization problem (32)-(35) were computed using the numerical procedures discussed in § 3.3 with data typical of the Severn Estuary. The parameter values are given by

$$
\begin{aligned}
T &= 4.32 \; 10^4 \text{ s.} \\
\ell &= 5 \times 10^4 \text{ m.} \\
h &= 15 \text{ m.} \\
S &= 22.5 \; 10^4 \text{ m}^2 .
\end{aligned}
\tag{58}
$$

With this data $K = 12.96$ for the normalized problem, and the imposed tidal elevation is given by $f(t) = \cos 2\pi t$. The maximum discharge across the barrier depends on a_0 , which is typically in the range $0.1 \leq a_0 \leq 1$. The average power in watts is determined from

$$\overline{P} = \rho g S F_0^2 E(\alpha) . \tag{59}$$

Solutions were also obtained for other representative values of the parameters K and a_0 in order to examine the behaviour of the numerical procedures. In all tests it was found that Algorithm 2 was convergent and required less than twenty iterations to reduce the first order correction to the functional E to 1% of its value. Frequently the choice $\theta = 1$ was sufficient throughout the iteration. The solutions were also observed to converge as the discretization step $h \to 0$, in all examples. Typical solution curves are shown in Figure 5 for the data (58) with $a_0 = 1$ and $h = 1/400$.

The optimal <u>constant</u> control for the problem (32)-(35) is derived by Count [8] as $\alpha(t) \equiv 2\pi/K$ in the case $a_0 = 1$. This choice of $\alpha(t)$ was taken as the initial approximation for the iteration procedure, and the average power output for this case and for the time-dependent optimal solution could be compared. With the Severn data (58), for the constant controller we obtained

FIG. 5   MODEL II - Turbines only

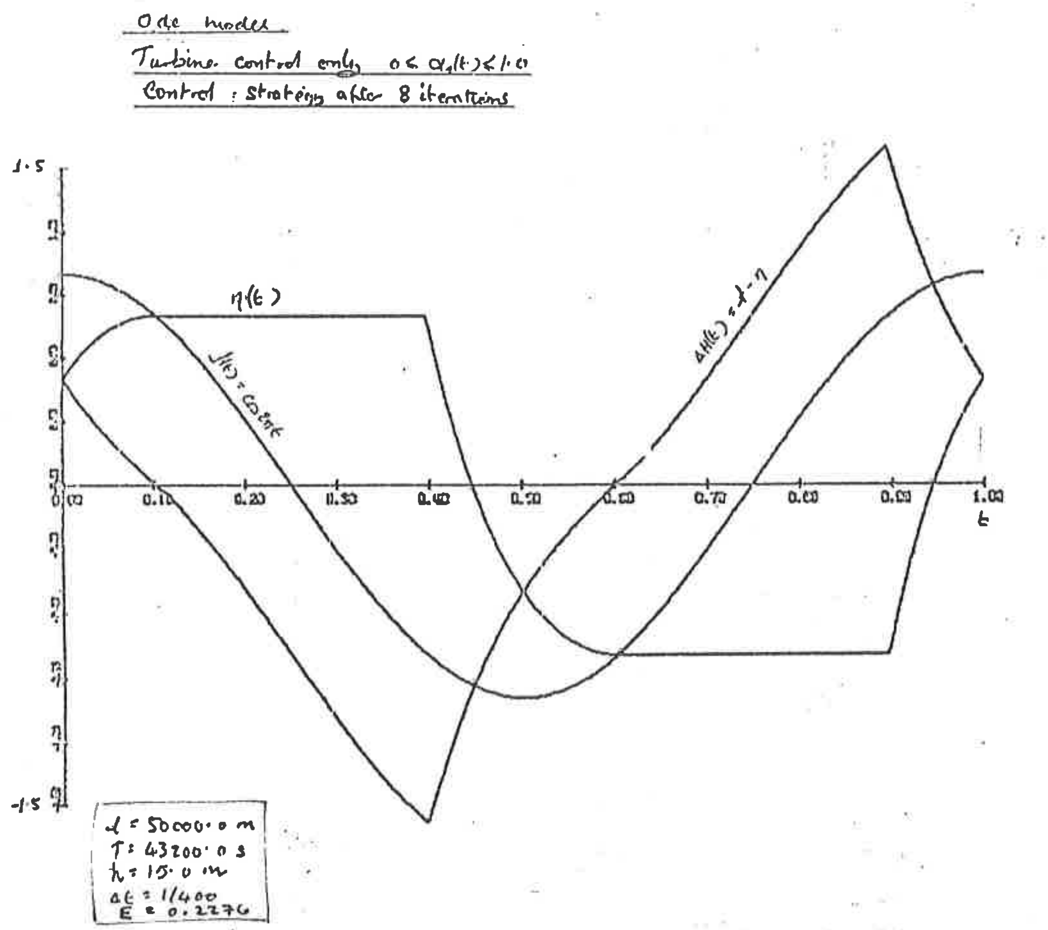

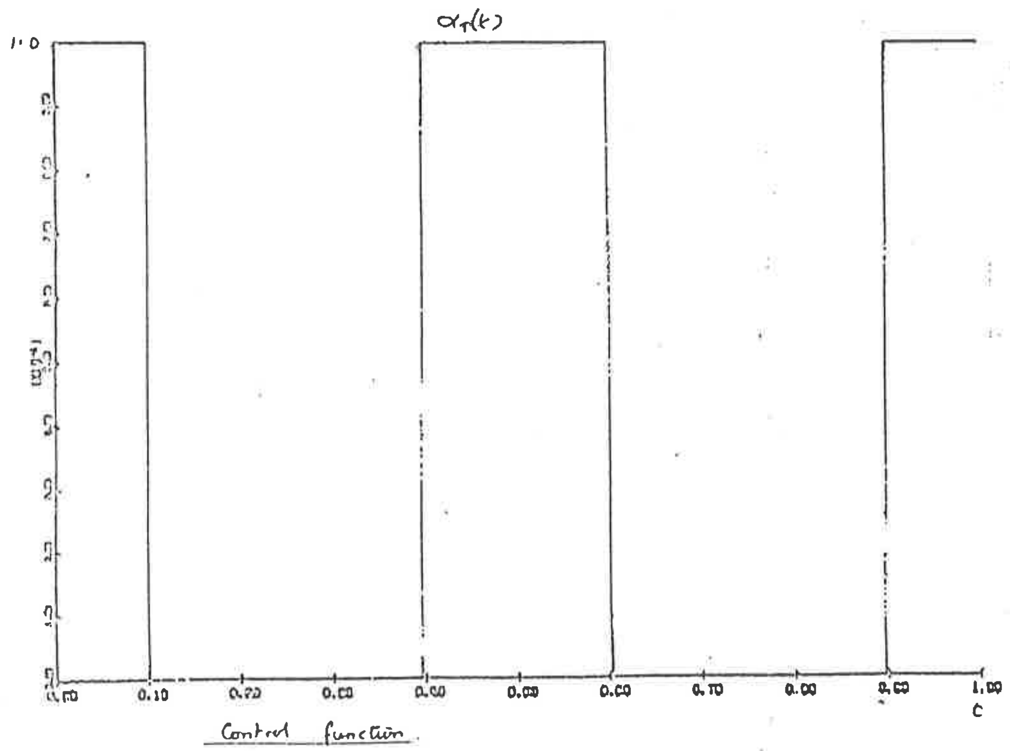

$E(\alpha) = 0.1212$, and for the optimal controller $E(\alpha) = 0.2276$. Using the optimal time-dependent control strategy thus gives an estimated improvement in the average power output from 7000 MW. to 12000 MW. with a tidal amplitude $F_0 = 5$m. For other choices of the data similar increases in power output were observed.

3.5 Generalizations

In practice the flow through a tidal barrier is controlled not only through turbines but also through sluices. Flow through the sluices contributes nothing to the instantaneous power developed but can be used to control the head difference across the barrier and so increase the average power output. To model the tidal power problem with both turbines and sluices we introduce two independent control functions $\alpha_1(t)$ and $\alpha_2(t)$ which determine the proportionate discharge across turbines and sluices, respectively, and are bounded such that

$$0 \leqq \alpha_1(t) \leqq a_1 \ , \qquad 0 \leqq \alpha_2(t) \leqq a_2 \ . \tag{60}$$

The influx velocity is then given by

$$u_0 = [\alpha_1(t) + \alpha_2(t)][f(t) - \eta(t)] \ . \tag{61}$$

Making the same assumptions as in the case of turbines only, the normalized power optimization problem becomes

$$\max_{\underline{\alpha} \in U_{ad}} E(\underline{\alpha}) = \int_0^1 \alpha_1(t) \ [f(t) - \eta(t)]^2 dt \ , \tag{62}$$

subject to

$$\dot{\eta} = (\alpha_1 + \alpha_2)K[f - \eta] \ , \tag{63}$$

$$\eta(0) = \eta(1) \ , \tag{64}$$

where U_{ad} is now the set of measurable two-dimensional vector functions $\underline{\alpha} = [\alpha_1, \alpha_2]^T$ satisfying (60) (a.e.).

The results of §3.2 are easily extended to the problem (62)-(64), and it can be shown that for any non-trivial $\underline{\alpha} \in U_{ad}$, there is a unique solution satisfying the system equations (63)-(64), that the responses η to (63)-(64) are uniformly bounded for all non-trivial $\underline{\alpha} \in U_{ad}$, and that an optimal control $\underline{\alpha}^* \in U_{ad}$ exists. The gradient function $\underline{\nabla E}(\underline{\alpha})$ is now given by

$$\underline{\nabla E}(\underline{\alpha}) = [(f - \eta)^2 + \lambda K(f - \eta), \quad \lambda K(f - \eta)]^T, \tag{65}$$

where the response satisfies the system equations (63)-(64) and the adjoint λ satisfies

$$\dot{\lambda} = [\alpha_1 + \alpha_2]\ K\ \lambda + 2\alpha_1[f - \eta]\ , \tag{66}$$

$$\lambda(0) = \lambda(1)\ . \tag{67}$$

Necessary conditions for the optimal are then

$$\alpha_i = \begin{cases} a_i & \text{if } \{\underline{\nabla E}(\underline{\alpha})\}_i \geq 0\ , \\ 0 & \text{otherwise,} \end{cases} \qquad i = 1, 2\ , \tag{68}$$

and the control is again "bang-bang" in nature.

In order to find numerical solutions to problem (63)-(68), Algorithm 2 is used with appropriate modifications to the state and adjoint systems and to the definitions of α^k, $\tilde{\alpha}^k$, and ∇E^k, which are now vector functions. The trapezoidal difference schemes and trapezium quadrature rules are applied to obtain the discretized algorithm, and the procedure remains stable and convergent.

Typical solution curves for the tidal power problem with both sluices and turbines are shown in Figure 6. Here $a_1 = 0.2$, $a_2 = 1.0$ and $K = 12.96$. It may be observed that for optimal power output the sluices are opened while the turbines are still operating, at the end of the power generation cycle. This result was not originally predicted. The average power output obtained is $\overline{P} = 0.1244\ \rho g S F_0^2$, which compares to $\overline{P} = 0.0894\ \rho g S F_0^2$ obtained with turbines only, assuming a corresponding value $a_0 = 0.2$ for the control constraint. We see that with the more sophisticated dual control system the energy generated can be further increased.

FIG. 6 MODEL II - Turbines and Sluices

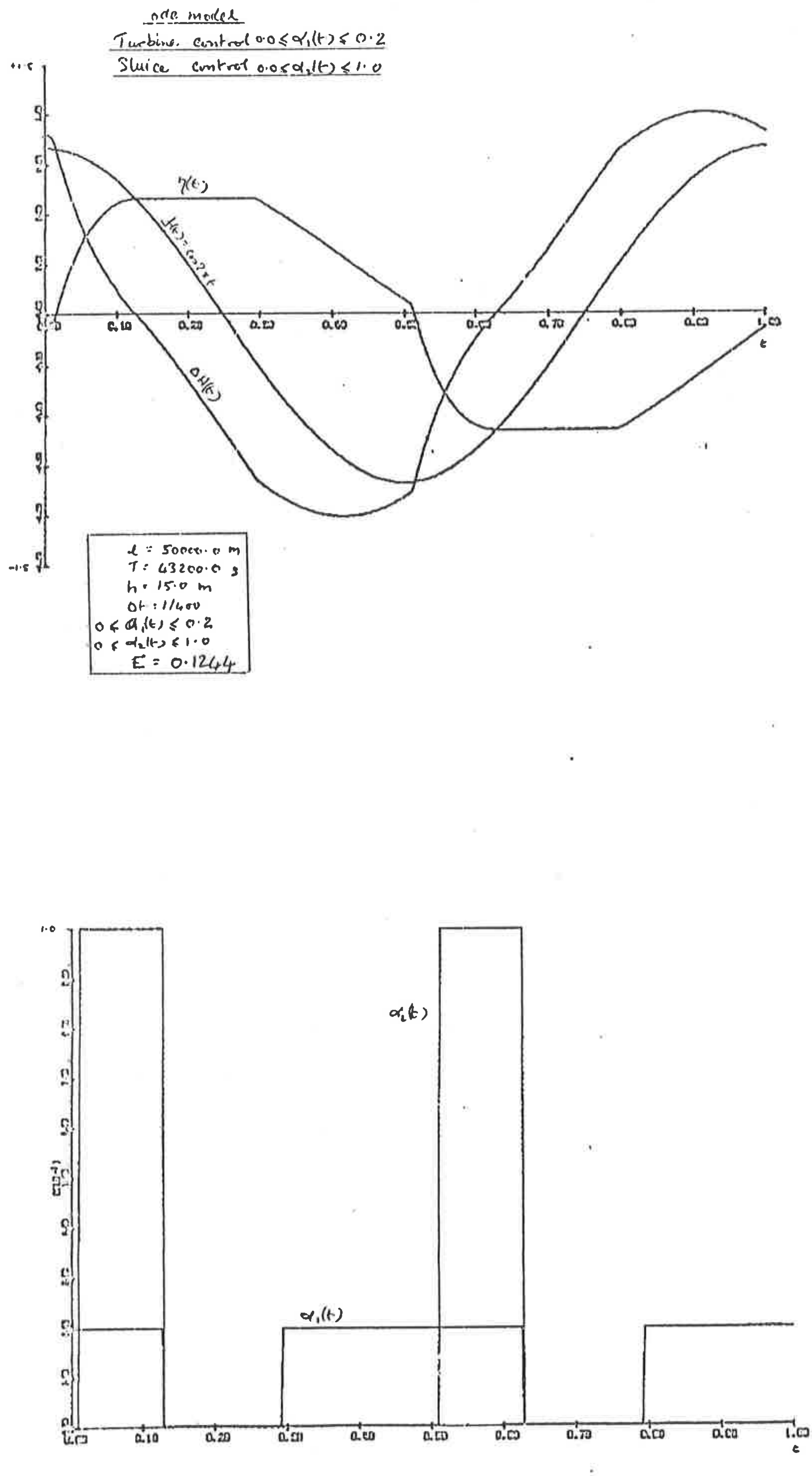

FIG. 7 MODEL II - Ebb Generation

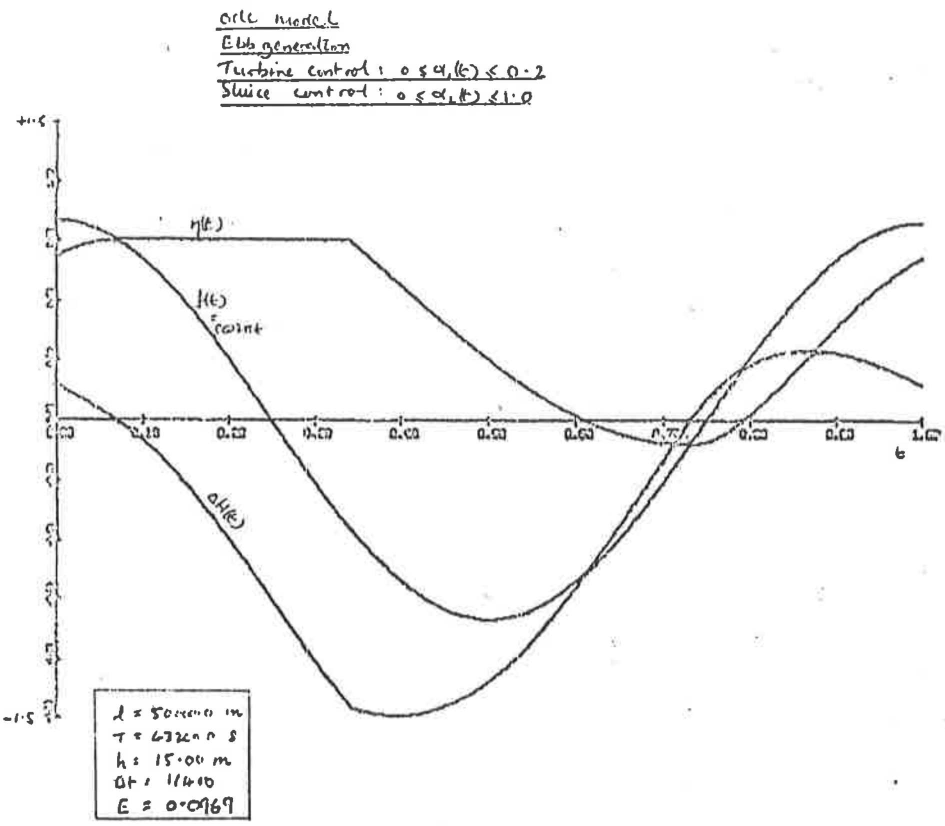

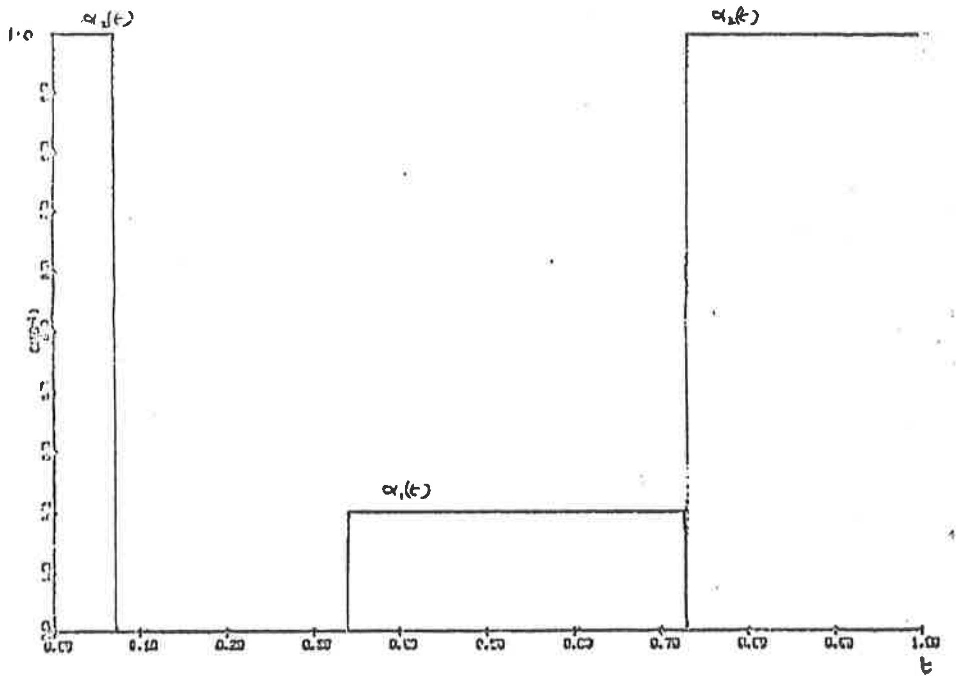

An additional modification to the tidal power problem can be made in order to model ebb-generation only schemes. Reversible turbines are in general less efficient and more expensive than one-way turbines, and it is arguable that power generation only during ebb tide periods may be more cost-effective than two-way generation. In the ebb generation only case, the influx velocity is defined by

$$u_0 = \alpha_1 H(f - \eta) + \alpha_2[f - \eta] , \tag{69}$$

where

$$H(s) = \begin{cases} s & \text{if } s < 0 , \\ 0 & \text{if } s \geq 0 , \end{cases} \tag{70}$$

and then the average power is proportional to

$$E(\underline{\alpha}) = \int_0^1 \alpha_1 H(f - \eta) [f - \eta] dt . \tag{71}$$

Using the conservation law as before, the optimal control problem is to maximize $E(\underline{\alpha})$ given by (71) subject to $\dot{\eta} = Ku_0$ and $\eta(0) = \eta(1)$.

Numerical results using an appropriate modification of Algorithm 2 for the ebb generation only scheme with both turbine and sluice controls are shown in Figure 7. Here $a_1 = 0.2$, $a_2 = 1.0$ and $K = 12.96$. The average energy developed by the ebb scheme is $\overline{P} = 0.0969 \rho g S F_0^2$, which compares to $\overline{P} = 0.1244 \rho g S F_0^2$ from the two-way scheme. The two-way scheme thus produces about 25% more power than the ebb scheme. We observe also that for the ebb scheme the sluices are operated essentially in isolation from the turbines.

3.6 Conclusions

We conclude that the optimal control theory technique developed for the linear-quadratic power generation problem associated with the oscillatory system of §2 can be extended to the more general non-linear tidal power problem and can be applied to a number of different models representing different energy production schemes. The results indicate that large increases in average power output can be achieved by using the optimal time-dependent control strategies to regulate flow through the tidal barrier. Estuarine dynamics have not been included in the models, however, and for realistic estimates of power output from various schemes, it is necessary to consider the effect of flow in the tidal basin on head differences at the barrier. In the next section we consider the application of optimal control theory to more general models incorporating dynamical behaviour in the basin.

4. MODELS III-IV - DYNAMIC SYSTEMS

4.1. The Model Equations

The energy generated by a tidal power station is directly dependent on the head difference between the water elevation on the seaward side of the tidal barrier and the surface elevation in the basin at the barrier. The latter is obviously influenced by the behaviour of the flow in the basin itself, and in order to obtain realistic estimates of power output from a tidal scheme, it is necessary to take into account the effect of dynamics in the basin. Mathematically the flow is treated as a function of both time and spatial position, and the system is described by a set of partial differential equations.

If we assume that the tidal basin is long relative to its depth, then the simplest one-space-dimensional model of flow in the basin is given by the linearized shallow water equations [21]:

$$\left.\begin{aligned} b(x)\eta_t &= -(A(x)u)_x \\ u_t &= -g\eta_x - pu/h(x) \end{aligned}\right\} \quad x \in [o,\ell] \qquad (72)$$

where $b(x) > 0$, $A(x) > 0$, $h(x) > 0$ are the mean breadth, mean vertical cross-sectional area and mean height of the channel, respectively, $\ell >> h(x)$ is the length of the channel, $g > 0$, $p > 0$ are gravitational acceleration and linear friction constants, respectively, $\eta(x,t)$ is the water elevation above mean height and $u(x,t)$ is the horizontal component of fluid velocity.

As in Model II (§3), we assume that the flow across the barrier (at $x = 0$) is controlled through turbines only, and that the influx velocity is proportional to the head difference between the surface elevation in the basin, $\eta(0,t)$, and the tidal elevation, $f(t)$, which is imposed on the seaward side of the barrier and is taken to be periodic with period T. At the upstream end of the basin (at $x = \ell$)

zero flow is assumed, and the boundary conditions are thus given as

$$\begin{aligned} u(0,t) &= \alpha(t)\ [f(t) - \eta(0,t)]\ , \\ u(\ell,t) &= 0, \end{aligned} \tag{73}$$

where the control function $\alpha(t)$ is bounded such that

$$0 \leqq \alpha(t) \leqq a_0\ , \quad \forall\ t \in [0,T]\ . \tag{74}$$

We also require that the functions η, u are periodic in time with period T, such that

$$\eta(x,0) = \eta(x,T)\ , \quad u(x,0) = u(x,\ T)\ . \tag{75}$$

The average power generated by the flow is now given by

$$\overline{P} = \rho g \frac{A(0)}{T} \int_0^T \alpha(t)\ [f(t) - \eta(0,t)]^2\ dt, \tag{76}$$

under the same assumptions as in the flat basin model (Model II).

The optimization problem is, as before, to find $\alpha(t)$ to maximize the average power $\overline{P}$, subject to the system equations (72) and boundary conditions (73) and (75). If we scale the variables with respect to time and space in order to obtain dimensionless quantities, then the optimal control problem may be written

$$\max_{\alpha \in U_{ad}} \quad E(\alpha) = \int_0^1 \alpha(t)[f(t) - \eta(0,t)]^2\ dt \tag{77}$$

subject to

$$\left.\begin{aligned} b(x)\eta_t &= -(A(x)u)_x \\ u_t &= -g\eta_x - \rho u/h(x) \end{aligned}\right\} \quad x \in [0,1],\ \ t \in [0,1]\ , \tag{78}$$

$$u(0,t) = \alpha(t)[f(t) - \eta(0,t)]\ , \quad u(1,t) = 0, \tag{79}$$

and

$$u(x,0) = u(x,1)\ , \quad \eta(x,0) = \eta(x,1)\ , \tag{80}$$

where the system coefficients ρ, g, $b(x)$, $A(x)$, $h(x)$ and the forcing function $f(t)$ now represent the normalized system data.

The choice of admissible controls must be considered with some care here. If the (non-trivial) function $\alpha(t)$ is sufficiently smooth, then for all sufficiently smooth initial data

$$\eta(x,0) = g_1(x), \quad u(x,0) = g_2(x), \tag{81}$$

the differential equations (78) with boundary conditions (79) have a unique continuous, differentiable solution, and we can show that the system (78)-(80) with periodic conditions, is well-posed (see §4.3). For less smooth control functions $\alpha(t)$, the initial value problem for equations (78)-(79) may possess only a weak solution and the necessary theory for the control problem is difficult to establish. We expect, however, that the optimal control must contain discontinuities, as in the simpler flat basin model of §3. Therefore, if we restrict the set U_{ad} to control functions sufficiently smooth to guarantee genuine solutions to the problem (78)-(80), then an optimal control maximizing $E(\alpha)$ and belonging to U_{ad} may not exist. On the other hand, if an optimal control exists which contains only a finite number of finite jump discontinuities, then we may approximate it as accurately as required by a smooth control function. We restrict our discussion, therefore, to bounded control functions which satisfy (74) and are "sufficiently smooth" for the initial value problem (78)-(79) and (81) to be well-posed. We consider as admissible controls only those functions which satisfy these conditions, or which are limits (in the L_2-sense) of such functions.

In practice the solution of the system equations (78)-(80) can be simplified considerably if it is assumed that the tidal basin is rectangular with constant mean depth h and breadth b. It is natural, therefore, to investigate first the model control problem (78)-(80) with constant coefficients (Model III) and then to examine the more difficult problem with variable coefficients (Model IV). The analysis of the optimization problem is essentially the same for both models, however, and we describe here the theory for the most general case.

4.2 Analysis of the Model

For any given "sufficiently smooth" (non-trivial) admissible control $\alpha(t)$, the system equations (78) together with boundary conditions (79) and (80) must have a unique solution, continuously dependent on the data, in order for the control problem to be well-posed. To show this it is necessary to demonstrate that the boundary conditions (79) are consistent with the hyperbolic system equations (78) and that the time periodic conditions (80) are natural to impose.

For consistency it is necessary that the boundary conditions provide a unique transfer of values from incoming to outgoing characteristics of the hyperbolic system at each boundary (see [14]). The characteristics for system (78) are given by

$$dx/dt = \pm\, c(x) \equiv \pm \sqrt{gA(x)/b(x)}\ , \tag{82}$$

where $c(x)$ represents the local wave speed, and the solutions of (78) are given by

$$\eta = (v + w)/\sqrt{g}\ , \qquad u = (v - w)/\sqrt{A/b}\ , \tag{83}$$

where the "canonical" variables $v = v(x,t)$, $w = w(x,t)$ satisfy (locally), along the characteristic lines, the equations

$$dv/dt = -p(v - w)/2h(x), \quad \text{along} \quad \dot{x} = +c(x)\ , \tag{84}$$

$$dw/dt = p(v - w)/2h(x), \quad \text{along} \quad \dot{x} = -c(x)\ .$$

(Here we have assumed dA/dx, db/dx are small compared to A, b and have neglected higher order terms locally). The values of v, w are therefore carried into and out from the boundaries along characteristic lines of positive and negative slope, respectively, and it is sufficient to show consistency of the boundary conditions (79) in terms of the canonical variables. The boundary condition at $x = 1$ is simply a reflection condition equivalent to $w(1,t) = v(1,t)$, and the boundary condition at $x = 0$ implies

$$v(0,t) = \Big((1-\sigma_0\alpha(t))w(0,t) + \sigma_0\sqrt{g}\alpha(t)f(t)\Big)/(1+\sigma_0\alpha(t)),$$

where $\sigma_0 = \sqrt{A(0)/gb(0)}$. The values of

$v(0,t)$ and $w(1,t)$ are therefore uniquely determined by the values of $v(1,t)$ and $w(0,t)$, for all t, as required.

The time periodic conditions (80) effectively replace the normal initial conditions associated with a hyperbolic system. To demonstrate that these conditions are natural to impose, in the sense that, in the limit as $t \to \infty$, the solution of the system equations (78), with any given initial state, converges to a unique "steady-state" periodic solution satisfying conditions (79), we use an iterative process similar to process (47) for computing solutions to the periodic ordinary differential problem describing the flat basin model (Model II). The iteration is given by

$$\underline{z}^{m+1}(0) = \underline{z}^{m}(1) \equiv G\underline{z}^{m}(0) , \tag{85}$$

where $\underline{z}(t) = [\eta(x,t),\ u(x,t)]^T$ is the solution of the problem (78)-(79) with initial date $\underline{z} = \underline{z}(0)$ at $t = 0$. If the operator G is a contraction, that is,

$$||G\underline{z}(0) - G\hat{\underline{z}}(0)||_s \leq K||\underline{z}(0) - \hat{\underline{z}}(0)||_s, \quad 0 \leq K < 1 , \tag{86}$$

where $||.||_s$ is a suitable norm on $L_2^2\ [0,1]$, (see [15]), then iteration (85) converges to a unique fixed point $\underline{z}^*$ such that the solution of problem (78)-(79) with initial data $\underline{z}(0) = \underline{z}^*$ satisfies $\underline{z}(1) = G\underline{z}^* = \underline{z}^*$ and is the required periodic solution satisfying (80).

To show that G is a contraction, for any given "sufficiently smooth" (non-trivial) admissible control $\alpha(t)$, we denote the difference between solutions to the initial-boundary value problem by $\delta\underline{z}(t) = \underline{z}(t) - \hat{\underline{z}}(t)$ and define

$$||\underline{z}(t)||_s^2 = \int_0^1 \left(b(x)\eta^2(x,t) + A(x)u^2(x,t)/g + k_\alpha(x)\eta(x,t)\right)dx, \tag{87}$$

where $k_\alpha(x) > 0$ has certain properties. (If $b'(x) \leq 0$ and has zeroes only at isolated points, then the choice $k_\alpha = \varepsilon\, b(x)$, where $\varepsilon \leq \min\{ \min_x \sqrt{A(x)/gb(x)}\ ,\ 4A(0)\int_0^1 \alpha(t)dt/(gb(0) + A(0)\int_0^t \alpha(t)dt)\}$ is sufficient.) We then obtain the inequality

$$\frac{d}{dt} ||\delta \underline{z}(t)||_s^2 \leq - Q_0 ||z(t)||_s^2 + Q_1(t) \ , \tag{88}$$

where $Q_0 > 0$ and $\int_0^1 Q_1(t)dt \leq 0$, and it follows that

$$||\delta \underline{z}(1)||_s^2 \leq e^{-Q_0} ||\delta \underline{z}(0)||_s^2 \ , \tag{89}$$

and, since G is linear, the condition (87) is satisfied with $K = e^{-Q_0}$.

We conclude that for all sufficiently smooth data the model system equations (78)-(80) are well-posed and we may sensibly look for a solution to the optimal control problem.

4.3 Necessary Conditions for the Optimal

Necessary conditions for the solution of the optimal control problem (77)-(80) are derived by the Lagrange technique. Pontryagin's Maximum Principle is not directly applicable to problems of this form with partial differential system equations. With sufficient smoothness conditions, however, the Lagrangian approach holds no difficulties.

The Lagrange functional associated with problem (77)-(80) is defined by

$$L(\alpha) = \int_0^1 \alpha(t)[f(t)-\eta(0,t)]^2 + \gamma(t)\big(u(0,t)-\alpha(t)[f(t)-\eta(0,t)]\big)dt \tag{90}$$

$$+ \int_0^1\int_0^1 \lambda(x,t)[-b\eta_t-(Au)_x] + \mu(x,t)[-u_t-g\eta_x-pu/h] \ dx \ dt \ .$$

Taking variations and using integration by parts, we can show now that the first variation of the Lagrangian is given by

$$\delta L(\alpha,\delta\alpha) \equiv \langle \nabla E(\alpha), \delta\alpha \rangle = \int_0^1 \Big\{ [f(t)-\eta(0,t)]^2 + A(0)\lambda(0,t)[f(t)-\eta(0,t)] \Big\} \delta\alpha(t)dt, \tag{91}$$

provided the state variables $\eta(x,t)$, $u(x,t)$ satisfy the system equations (78)-(80) and the adjoint variables $\lambda(x,t)$, $\mu(x,t)$ satisfy the equations:

$$\left.\begin{aligned} b(x)\lambda_t &= -g\mu_x \ , \\ \mu_t &= -A\lambda_x + p\mu/h \ , \end{aligned}\right\} \quad x \in [0,1], \quad t \in [0,1] \tag{92}$$

with boundary conditions

$$g\mu(0,t) - \alpha(t)A(0)\lambda(0,t) = 2\alpha(t)[f(t) - \eta(0,t)] \ , \ \mu(1,t) = 0 \ , \tag{93}$$

and

$$\lambda(x,0) = \lambda(x,1) \ , \quad \mu(x,0) = \mu(x,1) \ . \tag{94}$$

(We note that the adjoint equations are well-posed and solutions can be generated by an iterative process analogous to (85) (i.e. equivalent to (48) for Model II) using repeated backward integration.)

The higher order variations of the Lagrangian contain terms of order $O(\delta\alpha\delta\eta)$, $O(\alpha\delta\eta^2)$ and $O(\delta\alpha\delta\eta^2)$ and, as in the case of Model II, cannot be guaranteed to be of only one sign.

For the first variation to be non-positive for all admissible variations $\delta\alpha$, the optimal control $\alpha(t)$ must satisfy

$$\alpha(t) = \begin{cases} a_0 & \text{if} \quad \nabla E(\alpha) \equiv [f(t) - \eta(0,t)]^2 + \\ & \qquad A(0)\lambda(0,t)[f(t)-\eta(0,t)] > 0 \ , \\ 0 & \text{otherwise} \ , \end{cases} \tag{95}$$

and the control is expected to contain jump discontinuities at zeros of the function gradient $\nabla E(\alpha)$. Unlike the system of Model II, we can no longer guarantee that the optimal solution does not contain singular arcs, and in practice we find that there exist subintervals in time over which $\nabla E(\alpha) \equiv 0$ and the optimal control $\alpha(t)$ takes interior values in the constraint set $[0,a_0]$.

Existence of an optimal control cannot now be easily proved, as indicated in §4.1. An iterative process for determining a control which satisfies the necessary conditions can be constructed and shown to converge, however, as in the case of Model II.

4.4. Solution of the Optimal Control Problem

To determine an admissible control α with corresponding responses and adjoints satisfying the necessary conditions (78)-(80) and (92)-(95), we use first an iteration procedure equivalent to Algorithm 2 for the ordinary differential system of Model II. Given an approximation α^k to the optimal, this method produces a new approximation $\alpha^{k+1} = \alpha^k + \theta^k(\tilde{\alpha}^{k+1} - \alpha^k)$, where $\theta^k \in [0,1]$ and

$$\tilde{\alpha}^{k+1} = \begin{cases} a_0 \\ 0 \end{cases} \text{if } \nabla E(\alpha^k) \begin{cases} \geq 0 \,, \\ < 0 \,. \end{cases} \tag{96}$$

The selected control α^{k+1} is piecewise constant and is essentially "bang-bang" in nature. It can be shown theoretically that for some selection of the parameters θ^k this procedure converges, and, in practice, it is found that a discretized form of the algorithm does converge, although slowly, provided the parameters θ^k are small enough. A sample of the results for a case with constant system coefficients is shown in Figure 8 . Considerable high frequency oscillation can be observed in the controls and in the responses. These arise principally because the required control is not, in fact, "bang-bang", but is continuous and lies on the interior of the constraint set over a proportion of the time interval. The gradient $\nabla E(\alpha)$ should be identically zero on this subinterval, but the algorithm approximates it by a sequence of rapid and rather large oscillations about zero. This algorithm is not suitable, therefore, for the partial differential boundary control problem of Models III and IV, and a modified approach is required.

We consider now the gradient projection algorithm, in which the new approximation to the control is chosen as $\alpha^{k+1} = \hat{P}(\alpha^k + \theta\nabla E(\alpha^k))$, where $\hat{P}$ is the L_2 projection operator onto U_{ad}. The operator $\hat{P}$ is characterized by the property

FIG. 8 MODEL III - Algorithm 2

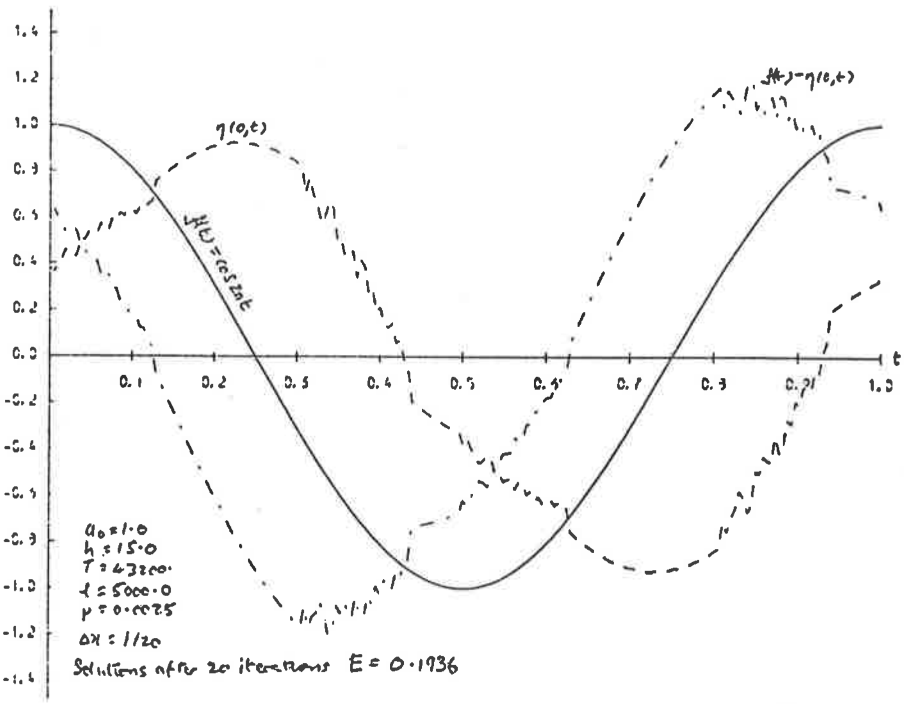

Application of the conditional gradient algorithm

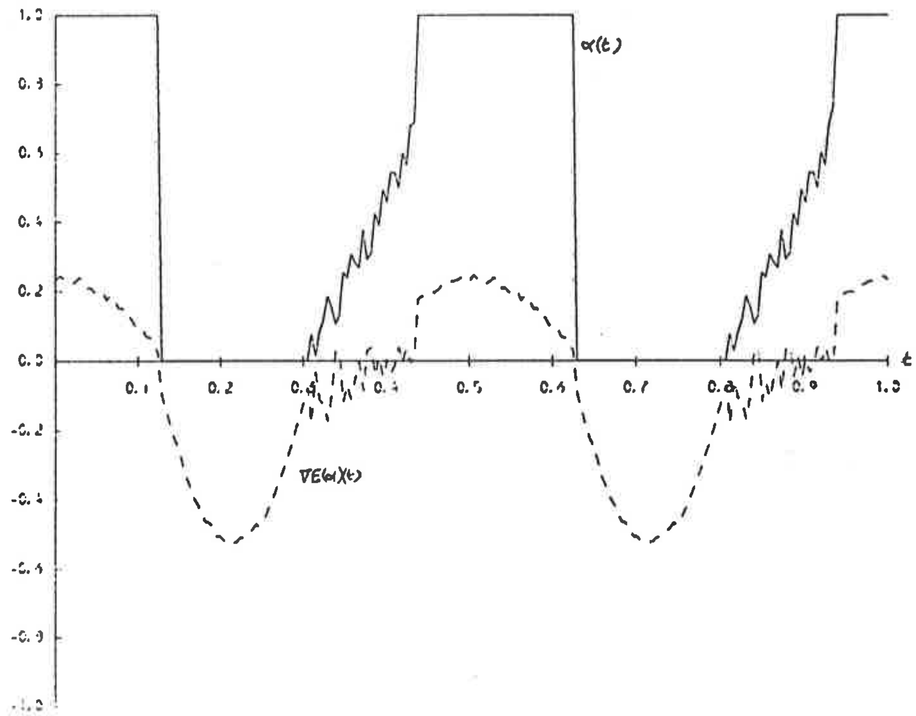

Application of the conditional gradient algorithm

$$\langle \hat{P}v - v,\ \hat{P}v - v \rangle = \min_{\alpha \in U_{ad}} \langle \alpha - v,\ \alpha - v \rangle , \tag{97}$$

or equivalently [18]

$$\langle v - \hat{P}v,\ \alpha - \hat{P}v \rangle \leq 0 , \qquad \forall\ \alpha \in U_{ad}. \tag{98}$$

For the selected control α^{k+1}, we have, therefore,

$$\langle \nabla E(\alpha^k),\ \alpha^{k+1} - \alpha^k \rangle \geq \frac{1}{\theta} ||\alpha^{k+1} - \alpha^k||_2^2 , \tag{99}$$

and it can be shown that for some choice of θ, $E(\alpha^{k+1}) \geq E(\alpha^k)$ [10]. If the initial approximation $\alpha^0(t)$ is continuous, then the algorithm generates a sequence of continuous controls α^k for which the functionals $E^k = E(\alpha^k)$ are monotonically non-decreasing, and provided an optimal solution exists amongst the admissible controls, the process converges and the limiting control satisfies the necessary conditions. The complete algorithm is described as follows:

<u>Algorithm 3</u>

<u>Step 1</u>. Choose $\alpha^0(t)$ continuous and such that

$$0 \leq \alpha^0(t) \leq a_0 , \quad \forall\ t \in [0,1].$$

Choose $\theta \in [0,1]$.

Set $E^0 := 0$, $\nabla E^0 := 0$.

<u>Step 2</u>. <u>For</u> $k := 0, 1, 2, \ldots$ <u>do</u>

<u>Step 2.1</u>. Set

$$\alpha^{k+1} := \begin{cases} a_0, & \text{if } \alpha^k + \theta \nabla E^k \geq a_0 , \\ 0 , & \text{" \quad "} \leq 0 , \\ \alpha^k + \theta \nabla E^k, & \text{otherwise} . \end{cases}$$

<u>Step 2.2</u>. Solve the state system (78)-(80) with $\alpha := \alpha^{k+1}$.

<u>Step 2.3</u>. Solve the adjoint system (92)-(94) with $\alpha := \alpha^{k+1}$.

<u>Step 2.4</u>. Set $E^{k+1} := E(\alpha^{k+1})$ using (77),

$\nabla E^{k+1} := \nabla E(\alpha^{k+1})$ using (95),

and $s^{k+1} := \langle \nabla E(\alpha^k),\ \tilde{\alpha}^{k+1} - \alpha^k \rangle$,

where

$$\tilde{\alpha}^{k+1} := \begin{cases} a_0 & \text{if } \nabla E(\alpha^{k+1}) \geq 0 , \\ 0 & \text{otherwise} . \end{cases}$$

Step 2.5. If $s^{k+1} < tol$ then goto Step 3.

Step 2.6. If $E^{k+1} \leq E^k$ then set $\theta := \theta/2$ and goto Step 2.1.

Step 2.7. CONTINUE

Step 3. Set $\alpha := \alpha^{k+1}$ and STOP.

4.5 Numerical Approximations

The numerical solution of the periodic-boundary value problem for the state system (78)-(80) in Step 2.2 of Algorithm 3 is obtained by a discrete analogue of the iteration process (85) described in §4.2. With discrete initial data given at points $x_j = j\Delta x$, $j = 0,1,..N$, for $t = 0$ and $t = \Delta t$, the system is integrated forward by a finite difference method (using steps of size Δt) to obtain solutions at $t = 1$ and $t = 1 + \Delta t$. The integration is then repeated using these solutions as initial data. The process is continued until the difference between the initial and final solutions at $t = 0$ and $t = 1$ is within same tolerance. The solution of the periodic adjoint system (92)-(94) in Step 2.3 is obtained by a similar iteration, using backward integration from discrete intial data given at $t = 1$ and $t = 1 - \Delta t$.

For Model III - the constant coefficient case - the method of characteristics is used to construct the finite difference approximations. The characteristics of the state system equations, given by (82), are straight lines in this case, and the canonical equations (84) can be integrated discretely by the trapezium method along the characteristics. If values for the canonical variables v and w are known at points (x_j, t_n) and $(x_j+\Delta x, t_n)$, then integration along the characteristics through these points gives expressions for the solutions at the point $(x_j+\frac{1}{2}\Delta x,\ t_{n+1})$ on the new time level $t_{n+1} = t_n + \frac{1}{2c}\Delta x$ where $c = \sqrt{gA/b}$ is the wave speed, in terms of the known values at time t_n. These expressions are solved together with (83) to give explicit finite difference approximations for the discrete values of η, u at each new time level, in terms of values at the previous time. (See [1] or [20].) Since the boundary conditions are consistent, the scheme simply transfers solutions directly from outgoing to incoming characteristics at the boundaries, and the numerical procedure is stable. For the adjoint system the characteristics are given by the same equations (82) as for the state system, and the same technique is used to give difference approximations for the discrete values of λ, μ at time level $t_n = t_{n+1} - \frac{1}{2c}\Delta x$, in terms of values at the time t_{n+1}. The backward integration procedure is also stable, and the complete scheme gives a second-order accurate method.

For Model IV - the variable coefficient case - the method of characteristics is unsatisfactory as the characteristic lines are now curved, giving a non-uniform difference mesh which is inefficient for computation. In this case we use instead a modified version of the Leap-frog method [20] to integrate the state and adjoint systems (78)-(80) and (92)-(94) on a uniform, staggered mesh. Straightforward application of the Leap-frog method leads to an unstable scheme due to the friction term $(-pu/h)$ in the momentum equation, but stability is restored by taking a time average of this term. Using a staggered mesh avoids certain difficulties in determining extra boundary conditions, but care must still be taken in approximating the conditions (79) and (93) in order to maintain stability of the procedure.

The difference approximations for the state system (78)-(80) are then given by

$$
\begin{aligned}
b_j(\eta_j^{n+1} - \eta_j^{n-1}) &= -\nu(A_{j+1}u_{j+1}^n - A_j u_j^n)\ , \quad j = 0,1,..N-1, \\
u_j^{n+1} - u_j^{n-1} &= -\nu g(\eta_j^n - \eta_{j-1}^n) - p\Delta t(u_j^{n+1} + u_j^{n-1})/h_j, \\
& \qquad\qquad j = 1,2,..N-1,
\end{aligned}
\qquad (100)
$$

with boundary approximations

$$u_0^n = \alpha^n[f^n - \tfrac{1}{2}(\eta_0^{n+1} + \eta_0^{n-1})] , \quad u_N^n = 0 . \tag{101}$$

The difference approximations for the adjoint system (92)-(94) are similarly given by

$$b_j(\lambda_j^{n+1} - \lambda_j^{n-1}) = - \nu g(\mu_{j+1}^n - \mu_j^n) , \quad j = 0,1,\ldots N-1,$$

$$\mu_j^{n+1} - \mu_j^n = - \nu A_j(\lambda_j^n - \lambda_{j-1}^n) + p\Delta t(\mu_j^{n+1} + \mu_j^{n-1})/h_j, \quad j = 1,2,\ldots N-1, \tag{102}$$

with boundary conditions

$$g\mu^n - \alpha^n A_0 \tfrac{1}{2}(\lambda_0^{n+1} + \lambda_0^{n-1}) = 2\alpha^n(f^n - \tfrac{1}{2}(\eta_0^{n+1} + \eta_0^{n-1})), \quad \mu_N^n = 0. \tag{103}$$

Here α^n approximates α at point $t = t_n$, η_j^n, λ_j^n approximate $\eta(x,t)$, $\lambda(x,t)$ at points $x = x_{j+\frac{1}{2}}$, $t = t_n$, and u_j^n, μ_j^n approximate $u(x,t)$, $\mu(x,t)$ at points $x = x_j$, $t = t_n$ (i.e. the finite difference meshes are staggered in the space dimension). The values of the system parameters are given by $b_j = b(x_{j+\frac{1}{2}})$, $A_j = A(x_j)$, $h_j = h(x_j)$, and $f^n = f(t_n)$. The difference mesh is defined such that $x_j = j\Delta x$, $j = 0,1,2,..N$, where $\Delta x = 1/N$. The time levels are defined by $t_n = n\Delta t$, $n = 0,1,...,$ where Δt is chosen such that the parameter $\nu = 2\Delta t/\Delta x$ satisfies

$$\nu^2 < \min_j \{b_j/gA_j\} . \tag{104}$$

The difference schemes (100)-(101) and (102)-(103) can be written in completely explicit form. Stability for values of the parameter ν up to the Courant-Friedrichs-Lewy limit of

$$\nu < \min_x \{1/c(x)\} = \min_x \{\sqrt{b(x)/gA(x)}\}$$

is established by considering discrete "energy" norms analogous to the continuous norm (87) (with $k_\alpha(x) \equiv 0$). Convergence of the iterative processes for determining the periodic solutions of the state and adjoint equations is similarly proved for the discrete problems with the same parameter value. A detailed analysis of the stability and convergence of the numerical procedures is given in [4].

The remaining steps, Step 2.1 and Step 2.4, in Algorithm 3 are discretized as in Algorithm 2 for the flat basin Model (Model II). The discrete approximations are all second-order accurate, and as the data and the solutions are all assumed to be smooth, we expect the discrete solutions to the optimization problem to converge asymptotically, with order two, as the mesh size $\Delta x \to 0$, with $\nu = 2\Delta t/\Delta x$ constant.

4.6 Results

The numerical procedures were tested with various data, in order to examine the bahaviour of the discrete algorithm. It was found that the iteration process converged reasonably rapidly and produced smooth solutions to the problem. If a suitable initial choice of θ was made, then θ generally remained constant throughout. The solutions were also found to converge as $\Delta x \to 0$ in all cases.

In order to make comparisons with the results of the flat basin model (Model II), and also the results of Count [8], data typical of the Severn Estuary was used with both the constant coefficient model (Model III), representing a rectangular channel of uniform depth, and the variable coefficient model (Model IV), representing an estuary with variable cross-section. The data for the constant coefficient case is given by:

$$
\begin{aligned}
b &= 1.5_{10}4 \text{ m} \\
h &= 15.0 \text{ m} \\
A &= bh \text{ m}^2 \\
P &= 0.0025 \text{ ms}^{-1} \\
T &= 43200.0 \text{ s} \\
\ell &= 5_{10}4 \text{ m} \\
a_0 &= 1.0 \\
f(t) &= F_0 \cos(2\pi t/T).
\end{aligned}
\qquad (105)
$$

Typical solution curves are shown in Figure 9.

The estimated average power output is now $\overline{P} = 0.194\ \rho gA(0)F_0^2$ which compares to $\overline{P} = 0.228\ \rho gA(0)F_0^2$, obtained with the optimal time-dependent control in the simple flat basin model, and $\overline{P} = 0.121\ \rho gA(0)F_0^2$, obtained with the optimal constant controller in the simple model. The predicted average in the more realistic model is reduced in comparison with the simple model, but still indicates that considerable improvements can be obtained by an appropriate control strategy.

For the variable cross section model, the same data is used, except that the basin is assumed to become narrower and shallower upstream of the barrier. The constants b and h are replaced by

$$b(x) = 1.5(1 - 0.8x)10^4 \text{ m}, \quad h(x) = 15(1 - 0.8x) \text{ m}. \tag{106}$$

The volume in the estuary basin is now reduced, and as expected, the average power output drops to $\overline{P} = 0.120\ \rho gA(0)F_0^2$. Solution curves are similar to those for the rectangular channel.

4.7 Generalizations

As for the flat basin model of §3, we may generalize the partial differential model to include dual control of both turbines and sluices, and to simulate ebb tide generation only.

For the dual control problem two independent bounded control functions $\alpha_1(t)$, $\alpha_2(t)$ are again introduced, which determine the proportionate discharge across turbines and sluices, respectively. The optimal control problem becomes

$$\max_{\underline{\alpha} \in U_{ad}} E(\underline{\alpha}) = \int_0^1 \underline{\alpha}_1(t)[f(t) - \eta(0,t)]^2 \, dt , \tag{107}$$

subject to differential equations (78), periodic conditions (80) and modified boundary conditions

$$u(0,t) = (\alpha_1(t) + \alpha_2(t))[f(t) - \eta(0,t)], \quad u(1,t) = 0. \tag{108}$$

The admissible controls $\underline{\alpha} = [\alpha_1, \alpha_2]^T$ are again assumed to be "sufficiently smooth" for solutions to the system equations to exist, and are required to satisfy

$$0 \leq \alpha_1(t) \leq a_1 , \quad 0 \leq \alpha_2(t) \leq a_2 . \tag{109}$$

The results of §§4.2-4.5 are easily extended to the modified problem. The gradient function $\underline{\nabla E}(\underline{\alpha})$ now becomes

$$\underline{\nabla E}(\underline{\alpha}) = \begin{bmatrix} [f(t) - \eta(0,t)]^2 + \lambda(0,t)A(0)[f(t) - \eta(0,t)] \\ A(0)\lambda(0,t)[f(t) - \eta(0,t)] \end{bmatrix} \tag{110}$$

where η, u satisfy the system equations (78), (80), (108), and λ, μ satisfy the adjoint equations (92), (94) and

$$g\mu(0,t) - \{\alpha_1(t) + \alpha_2(t)\}A(0)\lambda(0,t) = 2\alpha_1(t)[f(t) - \eta(0,t)],$$

$$\mu(1,t) = 0 . \tag{111}$$

Necessary conditions for the optimal then require that $\alpha_i(t)$ takes values 0 or a_i depending on the sign of $\{\underline{\nabla E}(\underline{\alpha})\}_i$, $i = 1,2$, except along singular arcs where the controls may take interior values on the constraint sets. Algorithm 3 is easily modified to solve the extended problem numerically.

For ebb generation only the average power is assumed to be proportional to

$$E(\underline{\alpha}) = \int_0^1 \alpha_1(t)H\{f(t) - \eta(0,t)\}\, dt, \tag{112}$$

and the influx velocity at the barrier is assumed to satisfy

$$u(0,t) = \alpha_1(t)\, H\{f(t) - \eta(0,t)\} + \alpha_2(t)\, [f(t) - \eta(0,t)] , \tag{113}$$

where the function $H(s) = s$ if $s < 0$ and $H(s) = 0$ if $s \geq 0$. Certain theoretical problems arise in reproducing the results of §§4.2-4.5 now, since the function $H(s)$ is not smooth at $s = 0$, and solutions to the adjoint system cannot be guaranteed to exist. However, $H(s)$ may be replaced in practice by a smooth approximation which is as close to H as required for accurate numerical solutions.

Numerical results for the two-way and ebb generation dual control schemes are shown in Figures 10-11 for the rectangular channel with data (105) (Model III). The average power generated is shown in Table 4 for the two-way and ebb schemes, and also for the corresponding turbines only model. The two-way scheme again produces about 25% more power than the ebb scheme, and the dual control scheme, with turbines and sluices, is clearly more effective than the turbines only scheme. Also shown in Table 4 are the results from Model II, the flat basin model, for the same three schemes. It can be seen that the results from the simple model are remarkably close to those of the dynamic model, differing in all cases by less than 10%. For Model IV, the variable coefficient case, the predicted average power outputs, given also in Table 4, are consistently lower than for the constant coefficient case, as expected. However, the same general conclusions can be drawn from the results.

Table 4 Average Power Production

	Scheme 1 Turbines only	Scheme 2 Two-way/Dual Control	Scheme 3 Ebb/Dual Control
Model II	0.089	0.124	0.097
Model III	0.082	0.115	0.092
Model IV	0.070	0.086	0.067

FIG. 9 MODEL III - Turbines only

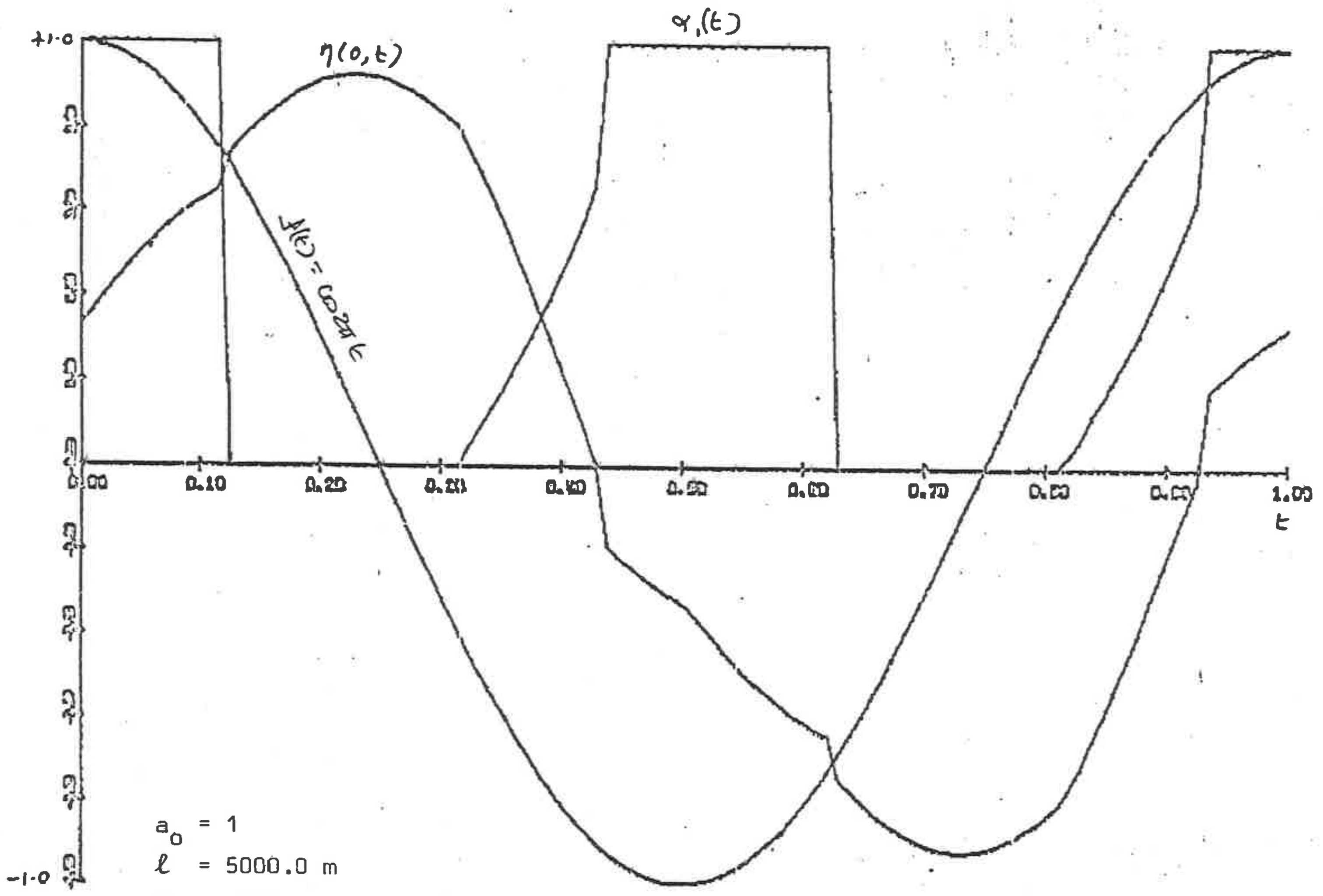

a_o = 1

ℓ = 5000.0 m

T = 43200 s

h = 15.0 m

p = 0.0025 ms^{-1}

Δx = 1/10

E = 0.1942

FIG. 10 MODEL III - Turbines and Sluices

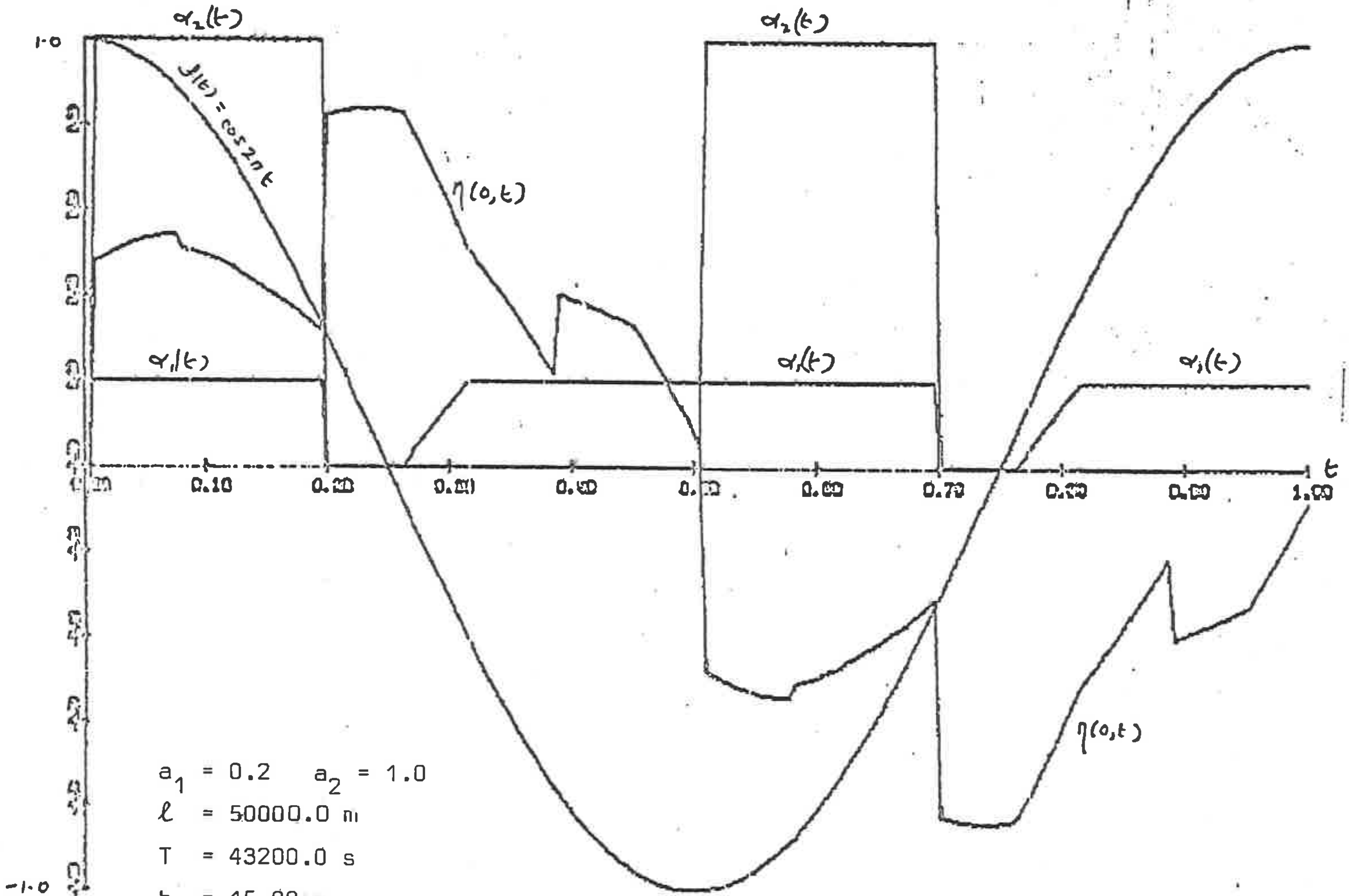

$a_1 = 0.2 \quad a_2 = 1.0$

$\ell = 50000.0$ m

T = 43200.0 s

h = 15.00 m

p = 0.0025 ms^{-1}

$\Delta x = 1/20$

E = 0.1146

FIG. 11 MODEL III - Ebb Generation

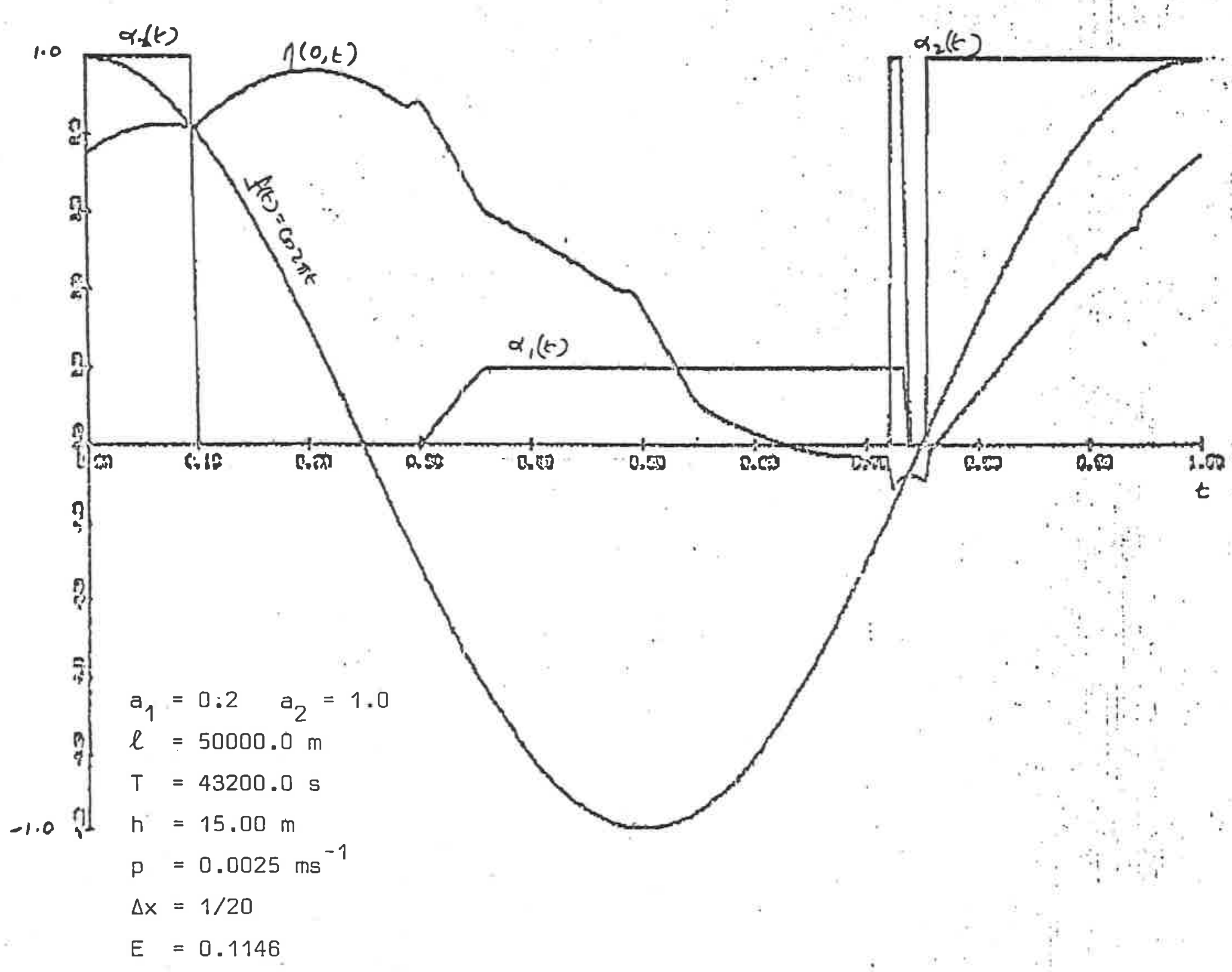

5. CONCLUSIONS

We examine here four general models of power generation schemes and develop techniques for determining the maximal average energy output of the schemes using optimal control theory. The first model provides a simple test example in which power is extracted from an oscillating system. The remaining models simulate tidal power generation from flow across a tidal barrage, with increasing degrees of sophistication. The second model, thus, treats only flow through the barrier, while the third and fourth models incorporate dynamics in the tidal basin, represented first as a simple rectangular channel, and then as a channel of variable cross-section.

The power generation problems are formulated as problems in optimal control, necessary conditions for the optimum are given, and numerical methods for computing solutions are developed. For the first model, which gives a classical constrained linear-quadratic control problem, a complete theory is derived, establishing the existence and "bang-bang" nature of the optimal and guaranteeing the stability and convergence of a fairly simple numerical procedure. The same theory is derived for the second model, but with greater difficulty. It is necessary first to establish that the system equations are mathematically well-posed, and, since the cost functional is no longer quadratic, a modification must be made to the numerical iteration scheme in order to obtain convergence. Inner iterations are also introduced in order to compute periodic solutions to the state and adjoint equations at each step of the procedure.

For these first two models the systems are represented by ordinary differential equations, and "bang-bang" controls with discontinuous switches are treated within the framework of the analysis. For the two remaining dynamic models, the systems are represented by a set of hyperbolic partial differential equations, and the behaviour of the system responses to discontinuous controls is difficult to predict. With sufficient smoothness assumptions it is shown that the system equations are well-posed, and necessary conditions for the optimal are derived. The optimal is not necessarily "bang-bang" now and may contain "singular arcs". Existence of a smooth optimal cannot be shown, but, providing a piecewise continuous optimal exists, the convergence of numerical schemes to a solution satisfying the necessary conditions as accurately as required is established. Modifications of the original numerical procedure, corresponding to that used for the second model, are needed to avoid oscillations in the control and system responses which now arise along the singular arcs.

Generalizations of all the models to systems with multiple controls are introduced and it is demonstrated that the theoretical and numerical techniques developed can be extended to a wide class of problems. Various power generation schemes are simulated, including both two-way and ebb tide generation schemes and schemes with dual controls for sluices and turbines in a tidal barrier. The principal conclusion reached is that with an appropriate control strategy the average power extracted from the generating source can be vastly increased. For the tidal power schemes, the introduction of both turbines and sluices gives an increase in power over schemes with turbines only, and two-way schemes give approximately 25% greater average energy output than ebb generation schemes (not accounting for loss of turbine efficiency). The incorporation of dynamics in the model reduces the predicted power production, but the estimates obtained from the simple model are reasonably close (within 10%) of those given by the dynamic model. The predicted optimal strategies are not altogether obvious, especially in the dual control case, and the results of the simulations also give valuable information concerning the control policies to be adopted.

We conclude that the optimal control approach to the tidal power generation problem is a feasible and attractive method for systematically computing flow control strategies, even for quite complicated dynamical models. Further studies are now being made using refined models with more accurate data in order to obtain more realistic power output predictions. Results have already been obtained for models which incorporate dynamics in the full estuary, eliminating the assumption that the elevation on the seaward side of the barrier is unperturbed by the flow across the barrier. Non-linear head-flow properties have also been incorporated. Details are given in [6]. To improve the model further, non-linear effects in the dynamic equations and two-dimensional phenomena must be taken into account. Extensions to these more realistic cases are now being made under the joint support of C.E.G.B. and S.E.R.C., and it is expected that a global optimization technique for the complete tidal power problem can be achieved by this approach.

6. REFERENCES

[1] Ames, W.F. (1977). Numerical Methods for Partial Differential Equations. 2nd Ed. Academic Press.

[2] Berry, P.E. (1982). On the use of the describing function technique for estimating power output from a tidal barrage scheme. CEGB Marchwood Engineering Laboratories, Technical Rpt. TPRD/M/1292/N82 TF425.

[3] Birkett, N.R.C. (1980). A study of an optimal power extraction problem. MSc Thesis, University of Reading, Department of Mathematics.

[4] Birkett, N.R.C. (1983). Optimal control of dynamic systems with switches. Ph.D. Thesis, University of Reading, Department of Mathematics.

[5] Birkett, N.R.C., Count, B.M., and Nichols, N.K. (1983). Optimal control problems in tidal power, J. of Dam Construction and Water Power, (to appear).

[6] Birkett, N.R.C., and Nichols, N.K. (1983). The general linear problem of tidal power generation with non-linear headflow relations. University of Reading, Department of Mathematics, Numerical Analysis Rpt. NA3/83.

[7] Bryson, A.E., and Ho, Y.C. (1975). Applied Optimal Control. Halsted Press.

[8] Count, B.M. (1980). Tidal power studies at M.E.L. CEGB, Marchwood Engineering Laboratories, Technical Rpt. MM/MECH/TF257.

[9] Gelfand, I.M. and Fomin, S.V. (1963). Calculus of Variations. Prentice-Hall.

[10] Gruver, W.A. and Sachs, E. (1980). Algorithmic Methods in Optimal Control. Pitman.

[11] H.M.S.O. (1981). Tidal power from the Severn estuary. Energy Paper No. 46.

[12] Jefferys, E.R. (1981). Dynamic models of tidal estuaries. Proc. of BHRA 2nd Int. Conf. on Wave and Tidal Energy.

[13] Keller, H.B. (1968). Numerical Methods for Two-Point Boundary Value Problems. Blaisdell.

[14] Kreiss, H.O. (1979). Numerical Methods for Partial Differential Equations. Ed. by S.V. Parter, Academic Press.

[15] Kreyszig, E. (1978). Introductory Functional Analysis. Wiley.

[16] Lambert, J.D. (1973). Computational Methods in Ordinary Differential Equations. John Wiley & Sons.

[17] Lee, E.B., and Markus, L. (1967). Foundations of Optimal Control Theory. John Wiley and Sons.

[18] Lions, J.L. (1971). Optimal Control of Systems Governed by Partial Differential Equations. Springer-Verlag.

[19] Pontryagin, L.S., Boltyanskii, V.G., and Gamkrelidze, R.V. (1962). The Mathematical Theory of Optimal Processes. Interscience.

[20] Richtmyer, R.D. and Morton, K.W. (1967). Difference Methods for Initial Value Problems. 2nd ed. Wiley Interscience.

[21] Stoker, J.J. (1957). Water Waves. Wiley Interscience.

[22] Wilson, E.M. et. al. (1981). Tidal energy computations and turbine specifications. Inst. of Civil Engineers Symp. on the Severn Barrage.